
DEVELOPMENT OF PHYSICS OF FAILURE BASED PROGNOSTICS FEASIBILITY TOOL FOR PREDICTIVE MAINTENANCE

**A thesis submitted to the University of Twente in accordance with
the requirements for completion of Master of Science degree in
Mechanical Engineering**

**By,
Karthikeyan Karuppusamy
s1972197**

December 18, 2019

**Dynamics Based Maintenance Research Group
Faculty of Engineering Technology
University of Twente**

SUPERVISORS

**Prof.dr.ir. Tiedo Tinga
Dr. Melissa M. Schwarz**

COMMITTEE

**Prof.dr.ir. Tiedo Tinga
Dr. Martin Luckabauer
Dr. Melissa M. Schwarz**

Abstract

Predictive maintenance is being exploited more in the current period due to its advantages over scheduled maintenance. In predictive maintenance, prognostics is used to estimate the Remaining Useful Life (RUL) of a component. Prognostics is classified into data-driven approach and physics-of-failure (PoF) approach. In the case of a data-driven prognostics approach, assistance is available in selecting a suitable algorithm that considers the available data's characteristics. In contrast, in a PoF prognostics approach, there is less assistance to select a failure model. High-level procedures do exist in PoF prognostics; however, they do not guide to select a failure model considering life cycle scenarios and feasible conditions within the failure mechanisms. When the procedures are applied within the literature, no justification is provided for the model selected, and the required monitoring techniques to utilise those models are neglected. Therefore a guidance is lacking in PoF prognostics to indicate when (old/new) to use a failure model and where (feasible conditions) to use a failure model.

To solve this, a feasibility tool is developed to aid users in identifying failure models and checking PoF prognostics feasibility. Due to the sheer volume of existing failure models when considering all the failure mechanisms, this research investigates a selected amount of failure models. To achieve this, failure models associated with identified failure mechanisms of a shaft are analysed. This analysis leads to a new proposed classification of failure models based on the methods of estimating the RUL. The new classification has been utilized in developing a flowchart, a guidance sheet, and a database, all of which together form the feasibility tool. The flowchart aids in checking the feasibility of PoF prognostics and guides in selecting the specific category of models depending upon the life cycle scenario of the component. The guidance sheet aids in identifying the respective feasible failure models from the database for a selected failure mechanism and loading scenarios. The database contains the models according to the new proposed failure model classification.

The flowchart, the guidance sheet, and the database are generic and can be customised for any component. To demonstrate the customizability of the tool, possible configurations of a shaft and the available monitoring techniques for a shaft have been analysed. Based on the results of this analysis, the feasibility tool has been customised for a shaft. In addition to the customizability demonstration, misunderstanding in shaft design has been discussed. As the dominant failure mechanism of a shaft is fatigue, the literature study on the fatigue models has aided in knowing the potential fatigue models for maintenance purposes.

Table of Contents

Acronyms.....	v
List of figures	v
List of tables	vi
Chapter 1. Introduction.....	1
1.1. Problem statement.....	1
1.2. Motivation and objective	2
1.3. Research question	3
1.4. Approach and outline	3
Chapter 2. Literature review	5
2.1. Shaft failure mechanisms and associated models	5
2.1.1. Fatigue models	6
2.1.2. Thermo-mechanical fatigue (TMF) models	9
2.1.3. Corrosion fatigue models	11
2.1.4. Fretting fatigue models	12
2.1.5. Creep failure	13
2.1.6. Conclusion on the aforementioned models.....	15
2.2. PoF prognostics procedures.....	16
2.2.1. Failure Modes, Mechanisms and Effects Analysis based prognostics approach	16
2.2.2. Selection of suitable components for Predictive maintenance	18
2.2.3. Discussion	19
2.2.4. Proposed approach to bridge the gap between failure models and Prognostics	19
Chapter 3. Development of feasibility tool	21
3.1. Nomenclature of failure models	21
3.2. Database.....	22
3.3. Guidance sheet.....	22
3.4. Flowchart.....	22
3.5. Working of feasibility tool	27
Chapter 4. Demonstration of the feasibility tool	29
4.1. Feasible models for a shaft.....	29
4.1.1. Possible models	29
4.1.2. Shaft sensors	30
4.1.3. Feasible models	32
4.1.4. Reasons for non-feasibility of other mechanisms.....	34
4.2. Customisation of feasibility tool for a shaft	34
4.3. Case studies	36

4.3.1. Spinner separator shaft	36
4.3.2. Composite beam tested in SLOWIND project	38
4.4. Misunderstanding in shaft design	39
Chapter 5. Discussion, Conclusion and Recommendations	41
5.1. Discussion on research questions	41
5.2. Potential models for fatigue in maintenance.....	42
5.3. Conclusion	42
5.4. Recommendations.....	43
References.....	45
Appendices	51

Acronyms

CDM	Continuum Damage Mechanics
DCA	Damage Curve Approach
DDCA	Double Damage Curve Approach
DLDR	Double Linear Damage Rule
FE	Finite Element
FMEA	Failure Modes and Effect Analysis
FMMEA	Failure Modes, Mechanisms and Effect Analysis
FRC	Fibre Reinforced Composites
LDR	Linear Damage Rule
LMP	Larson Miller Parameter
PHM	Prognostics and Health Management
PoF	Physics-of-Failure
RUL	Remaining Useful Life
TMF	Thermo-mechanical Fatigue

List of figures

Figure 1 Data-driven model selection chart from Matlab	1
Figure 2 Overview of RUL prediction models	2
Figure 3 General flow of existing procedures in PoF prognostics	2
Figure 4 Research approach	4
Figure 5 Shaft failure mechanisms and associated models	5
Figure 6 An example of crack growth plot	8
Figure 7 Phases of corrosion fatigue	11
Figure 8 Crack initiated in rotor hub due to fretting.....	12
Figure 9 Example for fretting modelling approach	13
Figure 10 Rupture curve with Larson Miller Parameter (33.7) for 9CrMoVNb steel	14
Figure 11 Stages of creep strain evolution.....	15
Figure 12 FMMEA based prognostics approach for new systems	17
Figure 13 FMMEA based prognostic approach for old systems	18
Figure 14 Flow methodology (Left-New component, Right-Old component)	23
Figure 15 Combined flow methodology for new and old components	24
Figure 16 Feasibility flowchart	26
Figure 17 Working of the feasibility tool.....	28
Figure 18 Deliverables of the shaft sensors	31
Figure 19 Axes representation for stress tensor in a shaft	32
Figure 20 Customised feasibility flowchart for shaft.....	35
Figure 21 Spinner separator assembly	37
Figure 22 Suitable position for torque cell.....	38

List of tables

Table 1 Shaft failure mechanisms - Causes	6
Table 2 Potential showstoppers in technical feasibility	19
Table 3 Nomenclature of models	21
Table 4 Step-by-step working procedure of the feasible tool.....	27
Table 5 Loading configurations in a shaft.....	29
Table 6 Possible cumulative life models for a shaft	30
Table 7 Possible condition-based models for a shaft.....	30
Table 8 Possible damage criterions for a shaft	30
Table 9 Shaft sensors.....	31
Table 10 Variables that could not be derived from the available sensors.....	33
Table 11 Guidance sheet for a shaft.....	33
Table 12 PoF prognostics Possibilities of a shaft (Only for new shaft).....	42

Chapter 1. Introduction

Maintenance costs money in the form of downtime, labour, tools, transportation, inventory, and capital. These factors make it vital to determine when maintenance action is required in advance. Prognostics is used in predictive maintenance to estimate how long it takes before a failure occurs in advance by estimating the remaining useful life (RUL) of the components. There are two different approaches used in prognostics, namely data-driven approach, and physics-of-failure (PoF) approach [1]. The data-driven approach uses operational system parameters and historical data of performance to create a model that links the operating system parameters to system degradation for RUL estimation. The physics-of-failure (PoF) approach uses the physical failure models that describe the behaviour of the system and combine the measured data with the physical model to estimate the RUL [1][2]. The measured data could be either usage, loads acting on the components, condition of the components, temperature or the environmental conditions.

1.1. Problem statement

As the data-driven approach requires knowledge of previous failure data to create a model, it is difficult to use this approach in a component without any previous failure data. On the other hand, the PoF approach could be used even without the previous failure data. However, one of the main challenges with the PoF approach is the selection of failure models. In the case of the data-driven approach, there is assistance, as depicted in **figure 1** to select a model based on the characteristics of available data [3]. In addition to that, there is numerous literature available on data-driven prognostics techniques and classification of failure models conditions [4]–[12]. On the other hand, there is hardly any assistance for PoF approach found in the literature to select a specific model. Apart from that, physical failure models are often indicated with a high level of complexity and not classified further. One such example is depicted in **figure 2** [13].

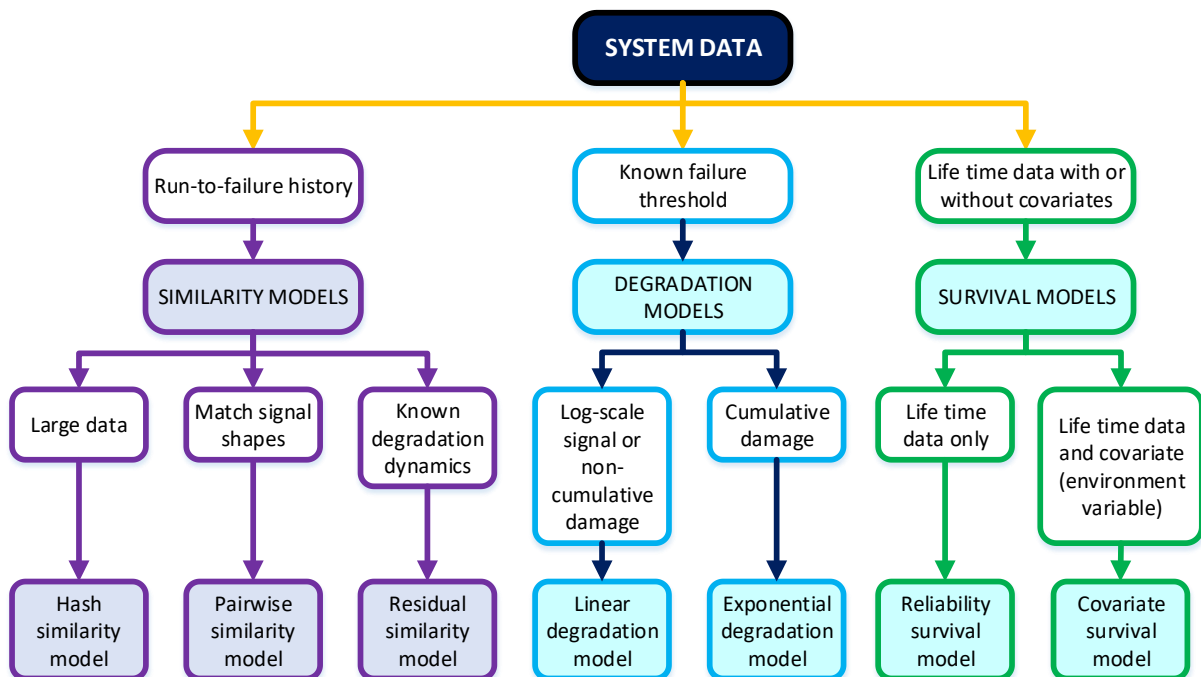


Figure 1 Data-driven model selection chart from Matlab [3]

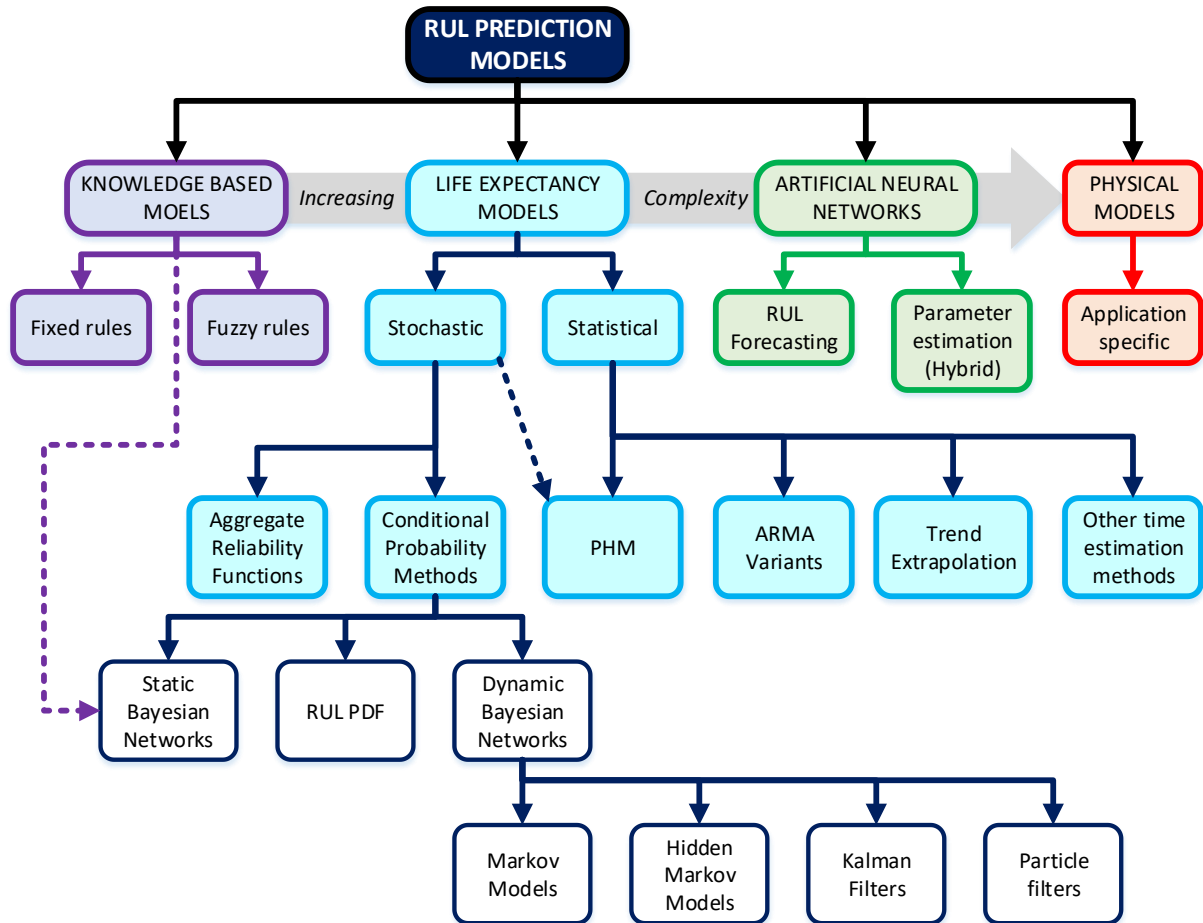


Figure 2 Overview of RUL prediction models [13]

However, there is literature in selecting components for predictive maintenance, and implementing PoF prognostics[14][15]. They are high level and lack to consider the life cycle scenarios (old component/new component) and feasible conditions within the respective failure mechanisms. Feasible conditions refer to the applicable conditions where a failure model may work. Example: nature of loading, material or environment.

The high-level procedures could be used only when there is a thorough knowledge of the failure mechanisms, models and sensors. These procedures are discussed in **section 2.2**. They follow the same general flow as depicted in **figure 3**, where the RUL is estimated after identifying the failure mechanism, failure model and a sensor as represented in the boxes. Each of these steps is extensive in terms of content. The studies that have utilised the procedures mentioned in **section 2.2** neither justify the selection of the failure model nor provide information on required monitoring techniques [16][17].

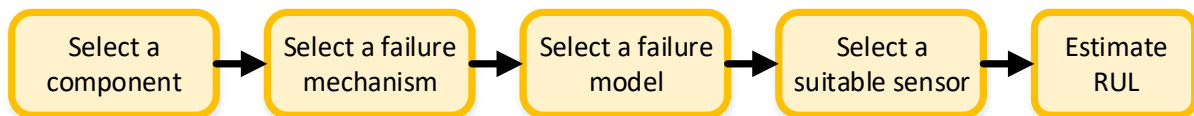


Figure 3 General flow of existing procedures in PoF prognostics

1.2. Motivation and objective

The initial goal was to make a modular PoF prognostics tool for rotating machinery. The deliverable of the tool would be the variables that have to be monitored for each component. It is essential to identify the models to know the variables. However, existing procedures and the studies that have

utilised those procedures did not aid in identifying feasible models. These challenges experienced in searching for the models demanded the objective to solve the issues in the identification of feasible failure models.

1.3. Research question

The following research question is proposed considering the objective mentioned in the previous section.

“How can identifying feasible failure models for PoF prognostics be approached considering life cycle scenarios and feasible conditions within the failure mechanisms?”

In addition to the main research question, some sub-questions that have to be considered.

1. What are the physical failure models available in the literature?
2. How could the failure models be classified based on the life cycle scenarios and feasible conditions within the failure mechanisms?
3. What are the variables used in the models?
4. What are the monitoring techniques available in the literature required for the variables used in those models?
5. How could this collected information on models and monitoring techniques be utilised to develop a tool that could aid in identifying the feasible models?

1.4. Approach and outline

Due to the sheer volume of failure models and numerous failure mechanisms, it is difficult to analyse all the available models. As this research was started in the rotating machinery, analysing the models and monitoring techniques for a typical rotating component would be beneficial. Therefore the shaft is selected as the case study component. This would also aid in checking the feasibility of PoF prognostics in a shaft apart from developing the tool. In addition to that, there could be different monitoring techniques depending upon the application for a variable used in a model. Therefore the tool has to be developed in a generic way that it could be customised for any specific component of interest. To demonstrate the customizability of the tool, a component has to be selected as the case study. The customisation is done for the shafts based on the identified feasible models for a shaft. Based on this approach, the thesis is structured as depicted in **figure 4**, and the outline of the thesis is explained as follows.

Chapter 2 – The failure mechanisms of shafts are identified, and the available failure models associated with the respective failure mechanisms are studied to know the different ways of estimating RUL, feasible conditions within those failure mechanisms and the applicability of the models to life cycle scenarios. In addition to this, existing proposed procedures are analysed to check if they could contribute to identifying the feasible models from the collected models, and gather inputs for the tool development.

Chapter 3 – This chapter deals with the development of the tool from the collected information in chapter 2. The developed tool is composed of three parts. They are the flowchart, the guidance sheet and the database. The process behind the development of the tool and the working of the tool are explained in detail in this chapter.

Chapter 4 – This chapter deals with the demonstration of the tool towards a specific component. Since the shaft is considered as the case study component, the available monitoring techniques for shafts are analysed to match with the variables in the models for the respective loading

configurations of shafts. Based on the results, the tool has been customised for shafts. In addition to customisation, the tool is used to identify feasible models for two applications.

Chapter 5 – This chapter covers the discussion on research questions, conclusion the recommendations for future research.

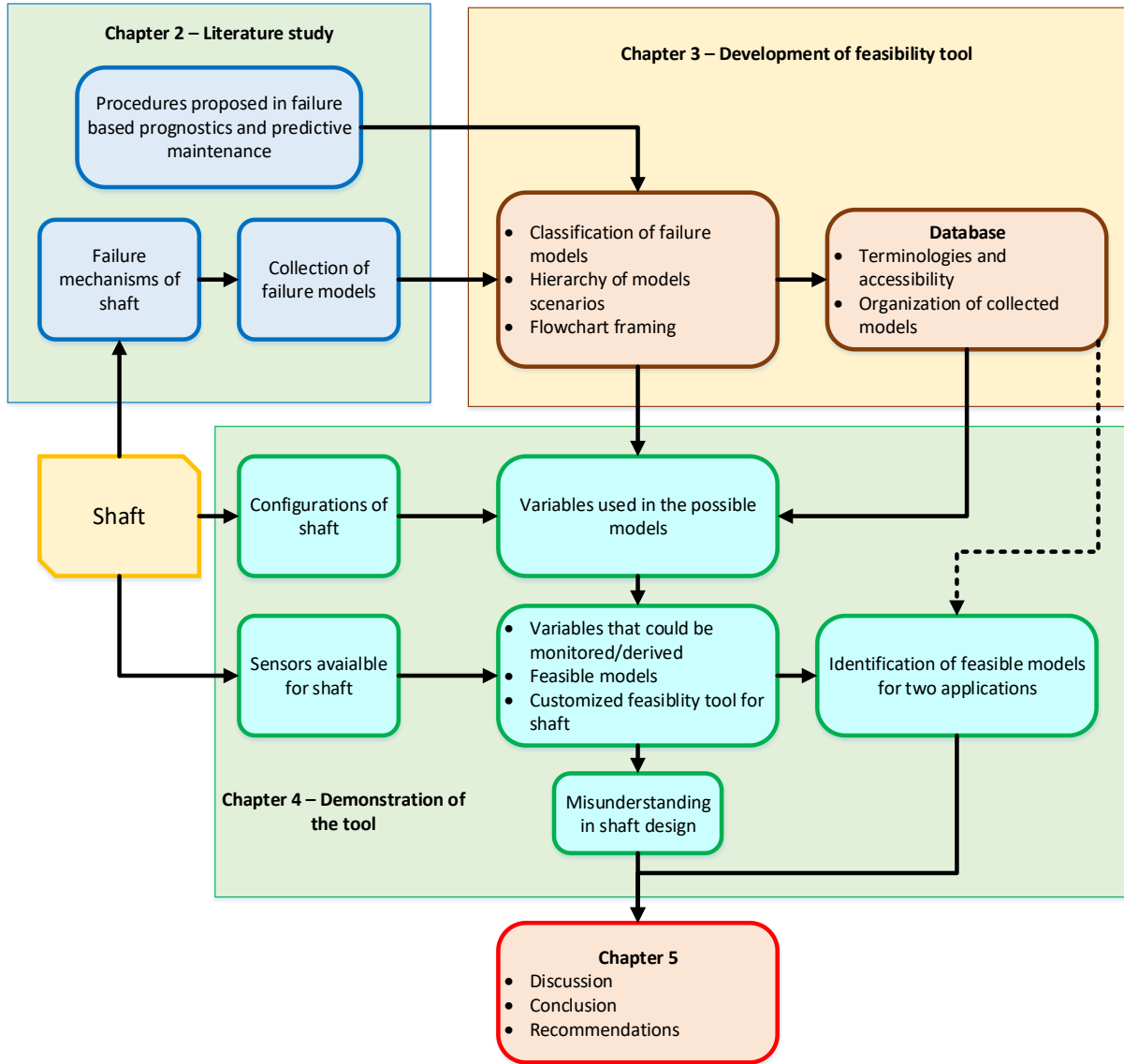


Figure 4 Research approach

Chapter 2. Literature review

This chapter covers the literature on failure models and existing procedures in PoF prognostics. In **section 2.1**, an investigation has been done on failure models to know the different methods of estimating RUL, feasible conditions for identified failure mechanisms, and the applicability of the models to the life cycle scenarios. This investigation is followed by a discussion on two PoF prognostics procedures in **section 2.2** to know how they work, and the missing things in identifying failure models.

2.1. Shaft failure mechanisms and associated models

A shaft is used either to transmit torque, act as axial support between two rotating elements like roller conveyors or both. The possible failure mechanisms of a shaft and the models associated with each of the failure mechanisms are depicted in **figure 5** to give an impression on overview of models. The cause of each failure mechanism is tabulated in **table 1**, along with some applications [18]–[20]. These models are discussed individually in the following subsections. Overloading failure or failure due to impact is not considered as it is not a degradation based failure. To give an impression on the variables used in the models and the method of calculating the number of cycles to failure, equations of the corresponding models are used in **subsections 2.1.1 to 2.1.5**.

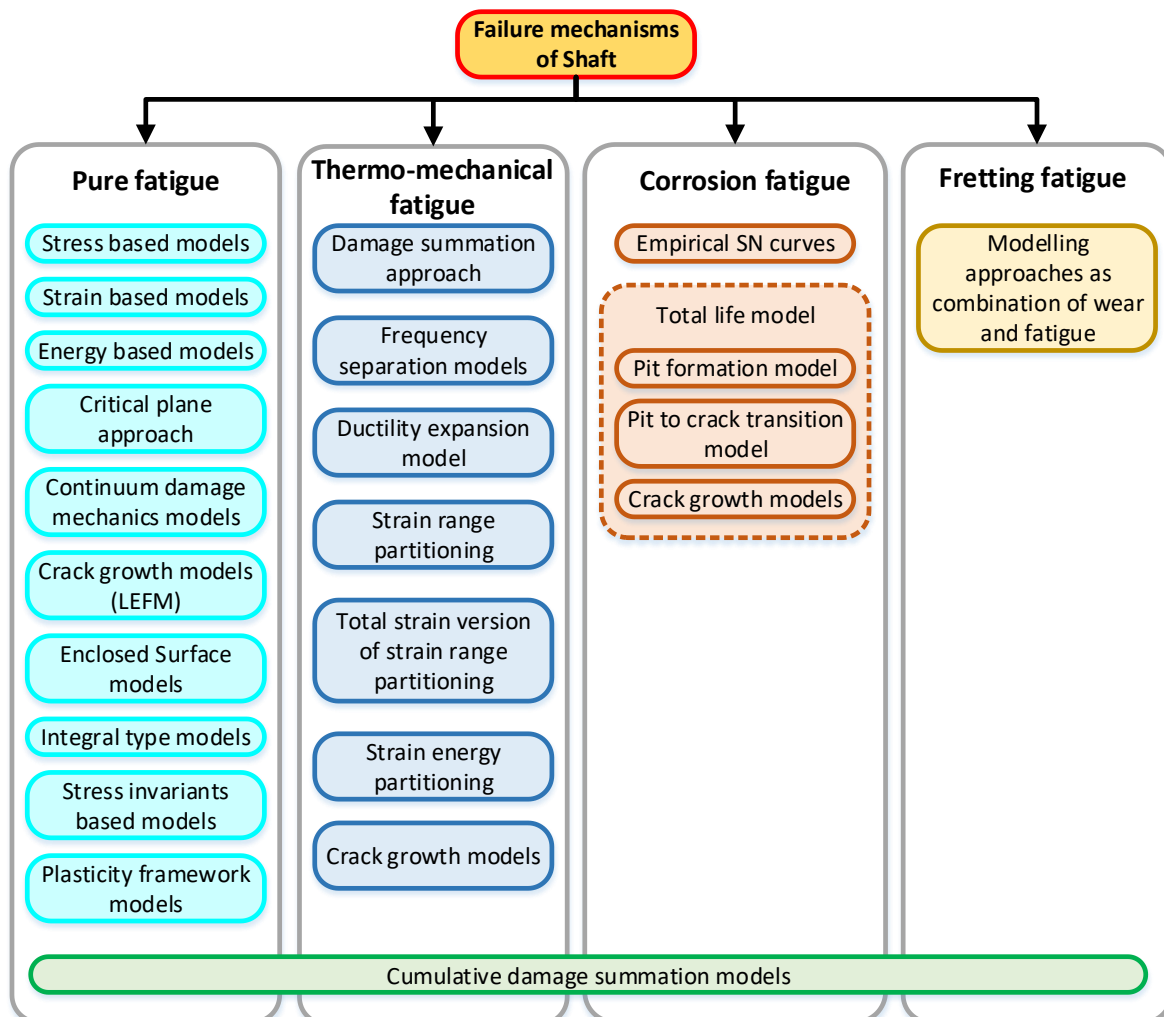


Figure 5 Shaft failure mechanisms and associated models

Failure mechanism	Causes	Applications
Fatigue	Cyclical loading in constant temperature and ideal environment (air)	Railway axles, wind turbine shafts, Electric motor rotor shafts
Thermo-mechanical fatigue (TMF)	Cyclical loading and alternating temperatures	Gas turbine shafts, crankshafts in Internal combustion engines
Corrosion fatigue	Cyclical loading in a corrosive environment	Shafts in submerged pumps, steam turbines
Fretting fatigue	Cyclical loading accompanied by minute relative motion	Any application with press-fit bearing, keys, splines

Table 1 Shaft failure mechanisms - Causes

2.1.1. Fatigue models

Stress/ strain/energy-based models

Stress/strain/energy-based models refer to the models that utilise the curve fitting equation from stress/strain/energy life curves, respectively. In the life curves, stress/strain/energy is plotted against the number of cycles to failure. Since the life curves are obtained for uniaxial loading conditions, respective authors have modified the uniaxial curve fitting equation according to their theory to account for multiaxial loading conditions. Therefore, these models turn out the number of cycles to failure for a given input value of stress/strain/energy parameters or a derivative of stress/strain/energy parameters, respectively.

The uniaxial curve fitting equations for stress/strain/energy life curves are represented in **equations 1, 3 and 5**, respectively [21]–[23]. An example of modification of each of those equations is represented in **equations 2, 4 and 6**, respectively [21][22][24][25]. The variable N in those models and the upcoming models in this thesis represents the number of cycles to failure.

$$\sigma_a = \sigma'_f (2N_f)^b \quad (1)$$

$$\frac{\Delta\tau_{oct}}{2} + \alpha(3\sigma_{h\ max}) = \sigma'_f (2N_f)^b \quad (2)$$

$$\varepsilon_a^t = \frac{\sigma'_f}{E} (2N_f)^b + \varepsilon'_f (2N_f)^c \quad (3)$$

$$\sigma_{n,max} \frac{\Delta\varepsilon_1}{2} = \frac{\sigma_f^2}{E} (2N_f)^b + \sigma'_f \varepsilon'_f (2N_f)^{b+c} \quad (4)$$

$$\Delta E_A = E_e (N_T)^B + E'_f (N_T)^C \quad (5)$$

$$(\Delta\tau\Delta\gamma) + (\Delta\sigma_n\Delta\varepsilon_n)_{max} = W'_e (N_T)^{Bs} + W'_f (N_T)^{Cs} \quad (6)$$

Cumulative damage summation models in fatigue

Stress/strain/energy based-models can only calculate cycles to failure for constant loading conditions. A separate model is required to calculate the accumulated damage due to variable amplitude loadings, and eventually estimate the RUL. Palmgren-Miner's linear damage rule (LDR) based on constant energy absorption theory, is one of the models used to calculate the accumulated damage. According to this rule, failure occurs when the damage ratio reaches unity. Damage ratio is

defined as the ratio of the number of cycles applied at a particular stress level to the number of cycles to fail at the same stress level. This model is represented in **equation 7** [26]. The main disadvantage associated with this model is that it does not take the effect of load sequence into account, thus showing failures at different damage ratios for low-to-high load and high-to-low load sequences. Despite this criticism, LDR is the widely used cumulative damage summation model as this does not require any constants and simple to calculate. Though there have been theories proposed in the later period to address this issue, it is less reported in the literature and less used [26].

$$D = \sum \frac{n_i}{N_i} = 1 \quad (7)$$

Constant amplitude loading applications do not require a cumulative damage summation model to estimate the RUL. However, prognostics is not required for the constant amplitude loadings, according to the author. This is because there is no requirement to monitor a parameter if none of the parameter is going to vary during the operation.

Damage Criterion

In addition to the models used for calculating the number of cycles to failure and accumulated damage, there are criteria to check the damage in stress/strain/energy-based category. Criteria could also be used to calculate the stress/strain/energy in multiaxial loading conditions, and the calculated stress/strain/energy could be substituted in the uniaxial curve fitting equations to calculate the number of cycles to failure.

Continuum damage mechanics (CDM) models

In the previously mentioned models, the number of cycles to failure is calculated from a separate model, and the cumulative damage for variable loadings is calculated from a separate model. Continuum damage mechanics approach combines the calculation of cumulative damage and cycles to failure as functions of each other [27]. A CDM model proposed by Chaboche is mentioned in **equation 8** [28]. On integrating **equation 8** with respect to the D and N, it results in equations for the number of cycles to fail and damage accumulation, as mentioned in **equations 9 and 10**, respectively. In addition to this, the non-linearity of the damage evolution is taken into account in CDM models providing an indirect measure of fatigue damage. This inclusion eliminates the issues with the effect of load sequence [27].

$$dD = [1 - (1 - D)^{\beta+1}]^{\alpha} \left[\frac{\sigma_{max} - \sigma_m}{M(\sigma_m)(1 - D)} \right]^{\beta} dN \quad (8)$$

$$N_F = \frac{1}{(\beta + 1)(1 - \alpha)} \left[\frac{\sigma_{max} - \sigma_m}{M(\sigma_m)} \right]^{-\beta} \quad (9)$$

$$D = 1 - \left[1 - \left(\frac{N}{N_F} \right)^{\frac{1}{1-\alpha}} \right]^{\frac{1}{1+\beta}} \quad (10)$$

The model proposed by Chaboche is only applicable for uniaxial loadings. However, in the later periods, numerous models have been proposed to account for multiaxial loading conditions.

Other models

Enclosed surface models, integral type models, stress invariants based models and plasticity framework models are the latest and least addressed models [24]. These models are rarely used due to their high demand in computational time and complexity associated with the solving, and they

also require a cumulative damage summation model to estimate RUL in case of variable amplitude loadings.

Critical plane approach

In critical plane approach, RUL is estimated in the similar way of using two separate models (a cumulative damage summation model and a model to calculate the number of cycles to failure) but with the help of finite element method. This approach is based on the idea that crack initiates on the plane where there is maximum damage in case of multiaxial loadings [29]. The plane with the maximum damage is called a critical plane. To find the critical plane, the damage is calculated in each plane with the finite element tool.

Crack growth models

In the previously mentioned approach, two separate models (a cumulative damage summation model, and a model to calculate the number of cycles to failure) are required to estimate the RUL. In crack growth models, the number of cycles to failure is calculated by integrating the crack growth between the instantaneous crack length and the critical crack length using the curve fitting equation of the crack growth plots. This approach is based on linear elastic fracture mechanics theory. And this approach of RUL estimation does not require a cumulative damage summation model and also the loading history.

The crack growth is plotted with stress concentration factor against crack growth rate on a log-log scale as depicted in **figure 6**, and the crack growth is classified into three phases based on the rate of propagation [30]. In the second phase, the crack growth is stable, and most of the available models are based on the crack growth rate in this phase. The crack growth is affected by stress ratio and directionality of the stresses. However, the slope remains constant for different stress-ratios, and a correction factor could be used to account for different intercepts. In addition to that, the stress concentration factor could be substituted similar to stress/strain/energy-based models to account for multiaxial loadings.

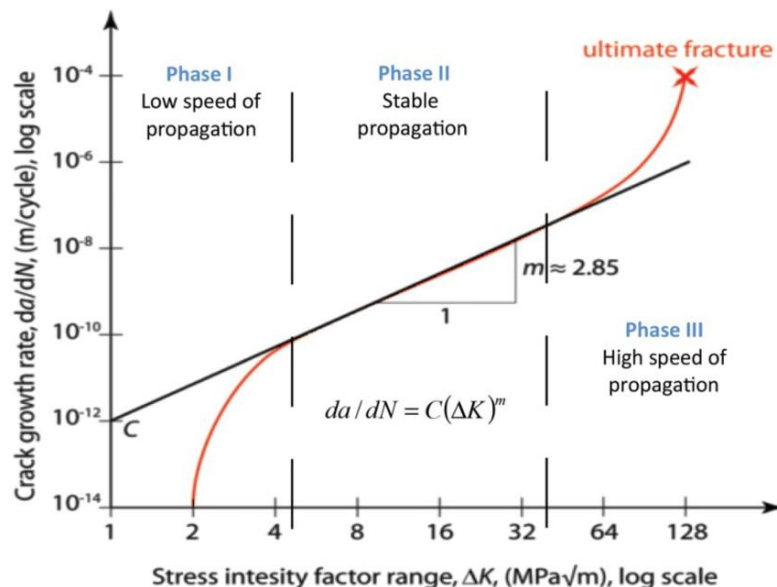


Figure 6 An example of crack growth plot[30]

Discussion and conclusion on fatigue models

1. Irrespective of the theory behind the derivation of a model, RUL is estimated in two approaches.

- i. The first approach requires two separate models (a cumulative damage summation model, and a model to calculate the number of cycles to failure) to estimate the RUL. This approach requires the entire loading history. Therefore, this approach cannot be used for machines that are already in service without any history on loading.
 - ii. The second approach (the crack growth models) directly estimates the RUL without an additional model and loading history. This approach requires only the forthcoming loads. Therefore, this approach could be used for both new components and old components.
2. Damage criterion could also be used in prognostics to check the presence of damage in old components before selecting a crack growth model. If the component is found to have no damage, then the damage criterion could be combined with a uniaxial curve fitting equation to calculate the number of cycles to failure.
 3. The feasible conditions for the models in fatigue failure are the directionality of the stresses (uniaxial, multiaxial proportional and multiaxial non-proportional) and the material. Since the current research has been focused on rotating machinery, a majority of models in this research are feasible for metals. The fatigue modelling of fibre-reinforced composites is different from that of the metals. However, the empirical SN curves and crack growth models are applicable for fibre-reinforced composites.
 4. The variables used in uniaxial models are uniaxial stress/strain/energy parameters, and the variables used in multiaxial models are derivatives of stress tensor or a combination of uniaxial strains and principal stresses.
 5. CDM models could be potential models for PoF prognostics. This is because there is no requirement to search for a separate cumulative damage summation model, and CDM models consider the effect of load sequence, and there are also models for multiaxial loadings.
 6. Since the critical plane approach could aid in locating the damage, it could be used for casings/housings where there are multiple loads.

2.1.2. Thermo-mechanical fatigue (TMF) models

RUL estimation in TMF is similar to that of plain fatigue. One approach requires two separate models to estimate the RUL, and the other approach (crack growth models) directly estimates the RUL. The difference among the models is the way of treating the damage caused by individual failure mechanisms of TMF.

Damage summation approach and ductility expansion model calculate the number of cycles to failure for fatigue and time to failure for creep individually as represented in **equation 11**[31]. The difference between the models is the method of solving fatigue and creep. For ductility expansion model, the number of cycles to failure caused by fatigue and creep are calculated using **equations 12** and **13**, respectively. For the damage summation approach, any model from fatigue and creep could be used. However, it should be noted that in the latest literature, the effect of oxidation has also been included by some authors as represented in **equation 14**[32].

$$\frac{1}{N_f} = \frac{1}{N_c} + \frac{1}{N_p} \quad (11)$$

$$\Delta\varepsilon_c N_c = D_c \quad (12)$$

$$\Delta\varepsilon_p N_p = D_p \quad (13)$$

$$\frac{1}{N_f} = \frac{1}{N_f^{fatigue}} + \frac{1}{N_f^{oxidation}} + \frac{1}{N_f^{creep}} \quad (14)$$

Frequency separation models, strain range partitioning model, total strain version of strain range partitioning and strain energy partitioning combine the effect of fatigue and creep. The frequency separation model uses a single strain parameter, as mentioned in **equation 15**[31][33]. The partitioning models partition the strain into four sections and calculate the number of cycles to failure for each section, as mentioned in **equation 16**[34]. Due to the similarity among the partitioning models, the strain range partitioning models is only mentioned in **equation 16**. The advantage of partitioning models over other models is its temperature independency.

$$N_f = C \Delta \varepsilon_{in}^{\beta} v_t^m \left(\frac{v_c}{v_t} \right)^k \quad (15)$$

$$\frac{1}{N_f} = \frac{F_{pp}}{N'_{pp}} + \frac{F_{cc}}{N'_{cc}} + \frac{F_{pc}}{N'_{pc}} + \frac{F_{cp}}{N'_{cp}} \quad (16)$$

Cumulative damage summation models in TMF

There is no cumulative damage summation model proposed exclusively for TMF. However, some of the models from the plain fatigue are found to be applicable for TMF[26]. In case of plain fatigue failure, there are models to account for the effect of load sequence. There is no such discussion in TMF failure to account for the effect of temperature sequence [35].

Crack growth models in TMF

The crack growth curves in TMF are plotted similarly to that of plain fatigue. However, they are more complicated. The crack growth in TMF is affected by stress-ratio, the phase difference between stresses and the phase difference between thermal and mechanical loading. Unlike plain fatigue, the slope of the crack growth curves varies for the difference in stress-ratio and the phase difference in loadings. For loadings with zero stress-ratio, the rate of crack growth decreases in the initial stage and then increases afterwards. For other stress-ratios, the rate of crack growth never decreases[36][37]. Due to this level of complexity, the literature found and the materials analysed are relatively much less in TMF compared to that of plain fatigue.

Discussion and conclusion on TMF models

1. RUL estimation in TMF is similar to that of RUL estimation in plain fatigue. One approach requires two separate models to estimate the RUL, and the other approach (crack growth models) directly estimates the RUL.
2. A combination of high temperatures and stress result in plastic strain. Therefore, the majority of the models utilise strain or derivatives of strain as the variable. The other variables include a derivative of stress, frequency of loading, temperature and drag stress.
3. Feasible conditions for TMF failure are the directionality of stresses (uniaxial, multiaxial proportional and multiaxial non-proportional) and the material. However, due to the complexity involved, the number of models available in the literature and the number of models considering the directionality of stresses are relatively less compared to that of the number of models in plain fatigue.
4. Among the models analysed, the strain range partitioning models are found to be advantageous over other models due to their temperature independency.
5. The importance of including the damage contributed by oxidation is still doubtful.

2.1.3. Corrosion fatigue models

RUL estimation in corrosion fatigue is similar to that of plain fatigue and TMF. One approach requires two separate models to estimate the RUL, and the other approach (pit/crack growth models) directly estimates the RUL.

The difference between the models in plain fatigue and corrosion fatigue is that the total life is divided into surface film breakdown, pit growth period, pit-to-crack transition period and crack growth period as depicted in **figure 7** and the cycles to failure for each period is calculated separately and added up as mentioned in the **equation 17** [38] [39]. However, no models have been found for the surface film breakdown period. In plain fatigue, only the crack growth models use integration based calculation to estimate the number of cycles to failure. In corrosion fatigue, all the models except the SN curves use integration. Therefore, they do not require a separate cumulative damage summation model. Because of this non-requirement, there is no cumulative damage summation model for corrosion fatigue except LDR.

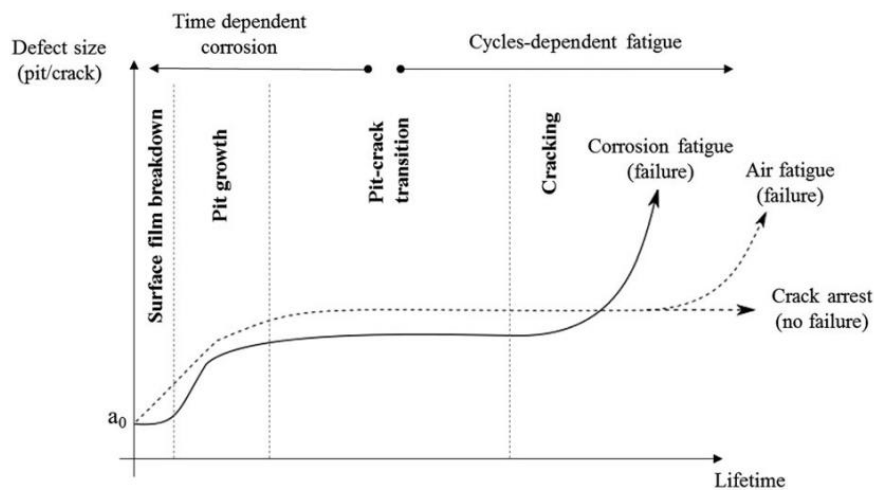


Figure 7 Phases of corrosion fatigue [38]

$$N_f = N_f^{pit} + N_f^{pit-crack} + N_f^{crack propagation} \quad (17)$$

Discussion and conclusion on corrosion fatigue models

1. RUL estimation in corrosion fatigue is similar to that of RUL estimation in plain fatigue. One approach requires two separate models to estimate the RUL, and the other approach directly estimates the RUL. There are cumulative damage summation models dedicated to corrosion fatigue.
2. The variables used in the models are stress amplitude, pit and crack dimensions, friction stress, pitting current and frequency.
3. Feasible conditions for corrosion fatigue are the directionality of the stresses (uniaxial, multiaxial proportional and multiaxial non-proportional) and the material.
4. In the industries where the corrosion fatigue plays an important role, no single procedure has considered corrosion fatigue as a single mechanism and mostly periodic inspections are conducted to check if the levels are within the thresholds [38]. The reasons quoted for this statement are
 - i. The complexity of the synergetic action between corrosion and fatigue

- ii. The applications encountering corrosion fatigue are large in the surface area subjected to corrosion.

2.1.4. Fretting fatigue models

Unlike corrosion fatigue or TMF, fretting fatigue only affects the crack initiation. It could be seen in interference fit shafts, dovetail joints in turbine blades (as depicted in **figure 8**), riveted plates, bearing races, pin joints, splined shafts and in places where there is a micro slippage (<100micrometer) between the contact surfaces [40][41]. The contact pressure and the minute wear give rise to crack initiation sites.

A majority of the literature focuses on modelling fretting fatigue, as depicted in **figure 9** [40]–[51]. Only one model has been found in literature as a single equation, where localised shear stress is used to calculate the number of cycles to failure. This model is mentioned in **equation 18**, and this model is similar to that of the stress-based model [51].



Figure 8 Crack initiated in rotor hub due to fretting[41]

$$\Delta\tau_{crit} = C_1(N_i)^{C_2} + C_3(N_i)^{C_4} \quad (18)$$

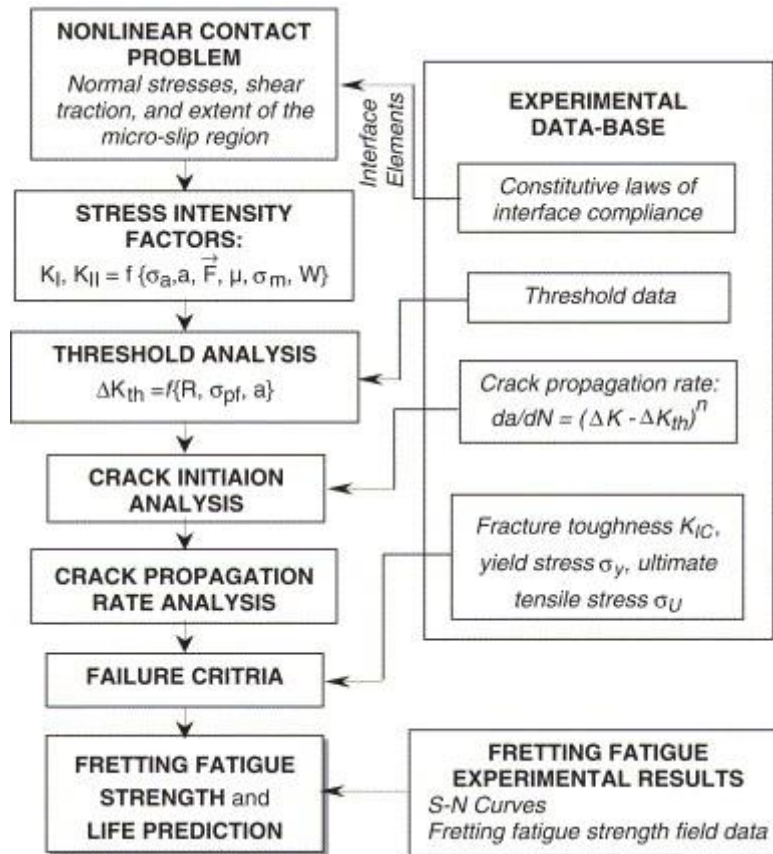


Figure 9 Example for fretting modelling approach [52]

Discussion and conclusion on fretting fatigue models

1. Only one model has been found in fretting fatigue, which is similar to the stress-based model in plain fatigue. The variable used in the model is localised shear stress.
2. As only one model is found, it is difficult to figure out feasible conditions for this failure mechanism.

2.1.5. Creep failure

Though creep is not an independent failure mechanism of shafts, the reason to study creep is due to the fact that the tool that is developed in this thesis should apply to any failure mechanisms.

Creep mechanism - Creep refers to the deformation of material over a long period under constant stresses, even below the yield strength. In general, creep is noticed when the temperature crosses 40% of its melting temperature approximately [53]. It should not be confused with instantaneous deformation due to impact force; rather, it is a time-dependent process. It should also be not confused with thermal expansion of metals, where a material deforms without any applied loads. The deformation is influenced by temperature, time, material properties and load. Notable applications include casings and high-temperature pressure vessels.

Creep models

There are two different curves used in RUL estimation of creep failure.

1. **Rupture curves** – Rupture curves are empirical curves in which the stress is plotted against a function of time and temperature. An example of a rupture curve is depicted in **figure 10**.

These curves are similar to the stress-based life curves (SN curves) in fatigue and turn out time to failure. In case of variable loading (different stress levels and different temperature levels), the damage accounted from each cycle could be estimated using Robinson's Life fraction rule as mentioned in the **Equation 19**, where the failure happens when the damage ratio reaches unity. The damage ratios defined as the actual time under particular stress and a particular temperature to the rupture time under the same stress and temperature [54]. There is no model found in literature accounting for the effect of temperature sequence in loading.

$$L_f = \sum_{i=1}^n \frac{t_i}{t_R(\sigma_i)} \quad (19)$$

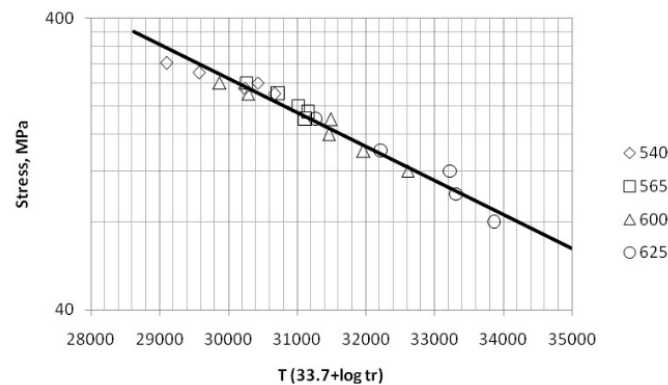


Figure 10 Rupture curve with Larson Miller Parameter (33.7) for 9CrMoVNb steel [55]

2. **Creep strain curves** – The creep strain is plotted against time in the creep strain curves. The creep strain evolution is divided into three stages (primary, secondary and tertiary) as depicted in **figure 11**. The creep strain rate is calculated using the curve fitting equations of these curves. There are numerous empirical curve fitting equations with minute differences [56]–[60]. One such model is mentioned in **equation 20**. The prediction of creep strain evolution by empirical models is better in the second stage, where the rate is almost stable. Apart from the empirical equations, there are two other major creep strain rate predicting models, namely theta projection models and continuum damage mechanics models mentioned in the following **equations 21 and 22**, respectively. The former is more complex and has more constants (20 constants) than the latter, which required ten constants [61][62]. Using the strain rate, the time taken to reach the desired deformation is calculated. The desired deformation is expressed as the percentage of strain. Therefore, these curves do not require loading history.

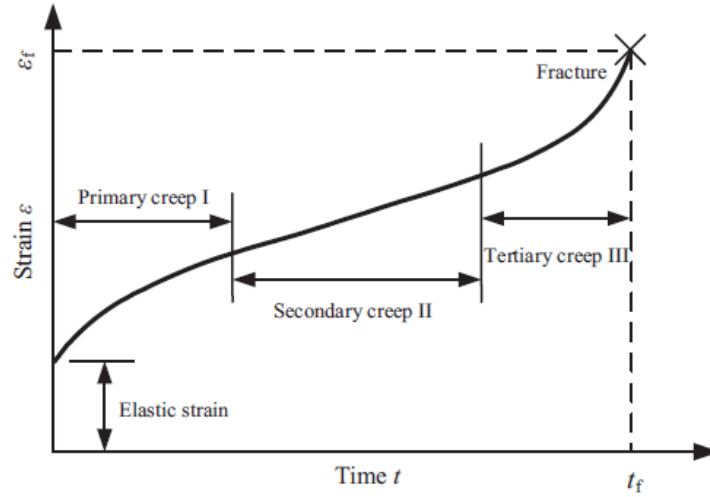


Figure 11 Stages of creep strain evolution [63]

$$\dot{\epsilon} = A \exp\left(-\frac{Q}{RT}\right) \sigma^n t^m \quad (20)$$

$$\dot{\epsilon} = \frac{d\epsilon}{dt} = \theta_1 \theta_2 \exp(\theta_2) + \theta_3 \theta_4 \exp(\theta_4 t) \quad (21)$$

$$\dot{\epsilon} = \dot{\epsilon}_0(D_d) \exp\left[-\frac{Q_d}{RT}\right] \text{Sinh}\left[\frac{\sigma(1-H)}{(1-D_p)}\right] \quad (22)$$

Discussion and conclusion on creep models

1. RUL estimation in creep is similar to that of plain fatigue. One approach requires two separate models to estimate the RUL, and the other approach directly estimates the RUL.
2. Variables are diverse in creep models. The most used ones are stress, temperature, time, strain rate and activation energy. Material is identified as a feasible condition.
3. It is found that the rupture curves are widely used amongst the engineers. There are two reasons quoted. The first reason is the risk of high variability in the creep strain plots making to use the creep strain plots only if known. Whereas in case of rupture plots, if there is a scatter, the lower bound could be used as a limit, and still, it's not a risk [55]. The second reason is the limited availability of creep strain plots [55].

2.1.6. Conclusion on the aforementioned models

1. From the models of previously discussed failure mechanisms, it is found that RUL estimation is done in one of the following two approaches.
 - i. Approach 1 – Two separate models are required to estimate the RUL. One model to calculate the number of cycles/time to failure and another model to calculate the cumulative damage caused by variation in the loadings. This approach requires the entire loading history. Therefore, this approach is applicable only for new components or components with the loading history. The variables used in the models in this approach correspond to the loads acting on the component and does not indicate the condition of the component. Some of the variables could be derived from the loads acting on the component.
 - ii. Approach 2 – The number of cycles/time to failure is obtained from a single model by integrating the curve fitting equation between the instantaneous value and the final

value. This approach applies to both old and new components. The models in this approach contain a variable that could be used to check the condition of the component. Example: Comparison of instantaneous crack length to the critical crack length. This approach applies to both old and new components.

2. The feasible conditions of the models for the respective failure mechanisms are as follows.
 - i. Fatigue, TMF and Corrosion fatigue – Directionality of the stresses and the material
 - ii. fretting fatigue – None
 - iii. Creep - Material
3. The number of models in synergetic failure mechanisms is relatively less compared to that of individual failure mechanisms.

2.2. PoF prognostics procedures

In this section, two methods focused on implementing PoF prognostics are analysed. The two methods are discussed individually in **subsections 2.2.1** and **2.2.2**. Though these methods have not been developed for failure model selection, they are discussed due to the following reasons.

1. A failure model is required to implement PoF prognostics in a component. Therefore, these procedures are studied to know the importance given to failure model selection.
2. There are no studies dedicated to failure model selection in PoF prognostics. Therefore the studies that have applied these procedures could be analysed to know the method of failure model selection.

2.2.1. Failure Modes, Mechanisms and Effects Analysis based prognostics approach

Failure Modes, Mechanisms and Effects Analysis (FMMEA) is a modified version of Failure Modes and Effects Analysis (FMEA)[64]. FMEA is used extensively in industries to identify the failures of a system and to take necessary actions to eliminate or mitigate the effect of failure. A limitation of the FMEA is that it does not give importance to the root cause of the failures. This limitation makes it less useful for understanding the loads and behaviour of the systems. To overcome this limitation, FMEA has been modified with an additional step of identifying the failure mechanisms for the respective failure modes, and an additional step of identifying failure models for the respective failure mechanisms.

Later, separate prognostic approaches for new and old components have been proposed. These approaches are depicted in **figures 12** and **13**, respectively and are explained as follows.

1. Prognostic approach for new components – This approach step by step by procedures. The initial step is FMMEA to identify the parameters for critical failure mechanisms. A selection of sensors follows this step and integrating those sensors. The final step or RUL estimation involves collecting and processing the data corresponding to the selected parameters.
2. Prognostic approach for old components – This approach is not entirely explained as it involves many steps. However, the main issues are explained.
 - i. It has been mentioned to install the available sensors and check the collected data for its usefulness. There is a second check for the relevant failure mechanism. The second check is contradictory as the information cannot be determined useful unless the relevant failure models are identified. And this could lead to erroneous data collection if the data is not useful after checking with the feasibility towards models.
 - ii. There are no alternatives provided for non-availability of data-driven/PoF models.
 - iii. The revision of sensors is done without identifying relevant failure models.

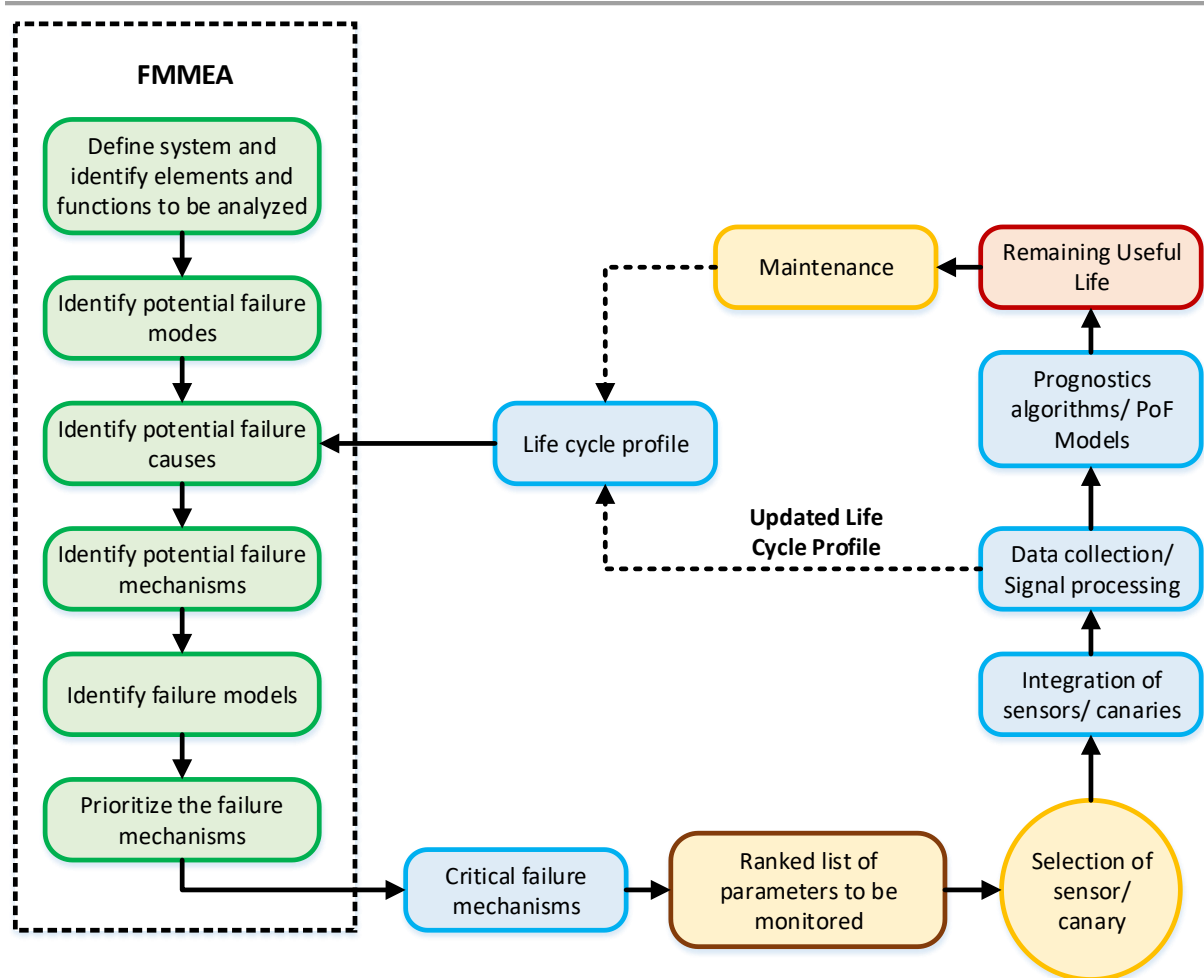


Figure 12 FMMEA based prognostics approach for new systems [14]

Studies that have applied this procedure

In the mechanical domain, the approach is not widely used, and only two works have been identified: a refrigerator compressor and a railway bogie [66][67]. They are discussed as follows.

- i. Compressor - The parameters to be monitored are directly established immediately after identifying the failure mechanisms and without identifying any failure models.
- ii. Railway bogie - Failure modes (fatigue cracks) are identified as failure mechanisms for some components, and no justification has been provided for the selected failure models. Paris law, Forman law, and spall initiation and progression models are selected for fatigue cases, but they are not correlated back to their components. Instead, a comparison is made amongst the selected failure models for its requirements and efficiency. In addition to that, there are no mentions about the techniques to monitor crack growth models in each respective component.

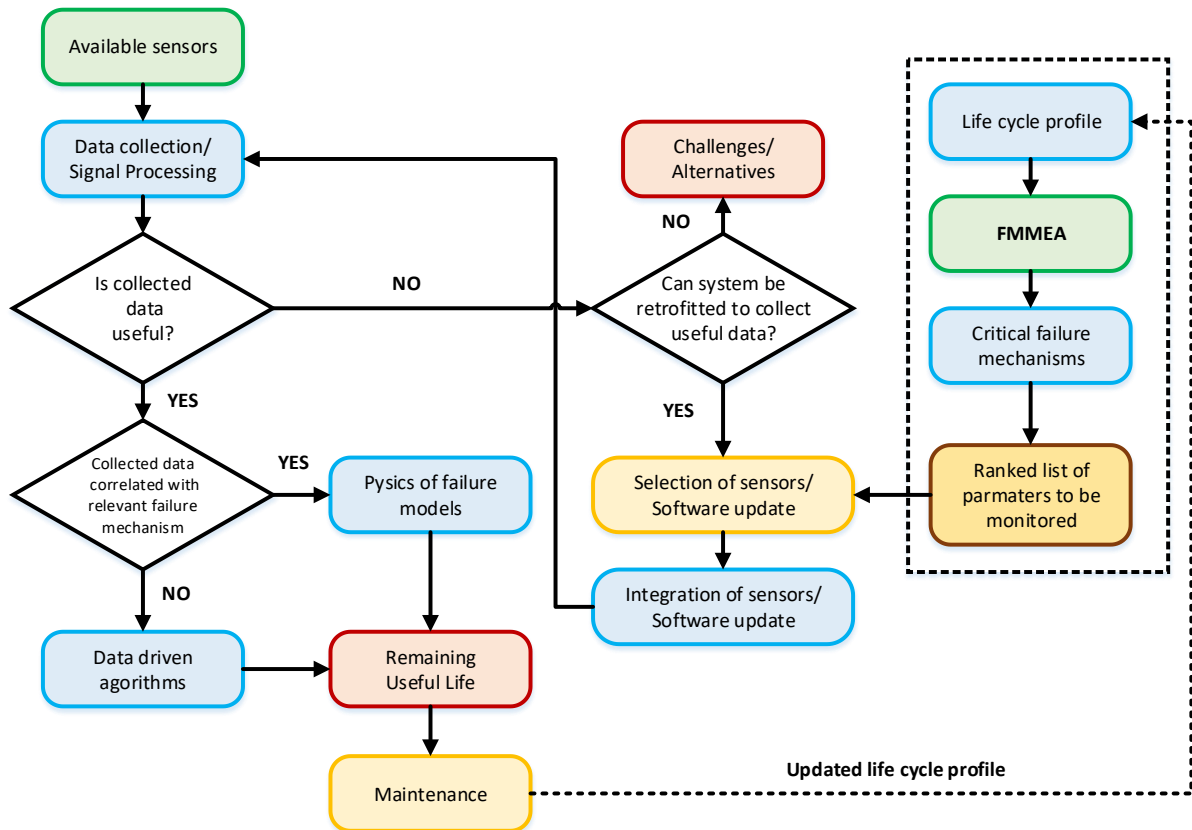


Figure 13 FMMEA based prognostic approach for old systems [14]

2.2.2. Selection of suitable components for Predictive maintenance

Tiddens has proposed a three-step procedure covering technical, economical, clustering and organisational factors for the selection of suitable components for predictive maintenance [15]. The three steps are criticality classification, showstopper identification and focused feasibility study. In the first step, the critical components are filtered by the four-quadrant method. The second step involves a feasibility check where showstoppers are considered. Showstoppers are potential factors that can make the prognostic approach infeasible or indicated there is no value in implementation. During the final step, the selected candidates are discussed against their economic and technical feasibility from a detailed perspective to make a final decision.

Since the first step is used only to reduce the number of components, it is not discussed here. Showstoppers include clustering, technical, economic and organisational factors. The technical showstoppers suggested in the procedure (t1a, t1b, t2a and t2b, are represented in **table 2**) are generic and encompass many factors into them. The factors include failure mechanism, respective failure models, monitoring techniques for the variable used in respective models, material properties used in the failure models, and computational tools to utilise the failure models if necessary. Instead, these factors are checked in the third step of the whole procedure titled as focused feasibility. This is quite contradictory because it is not possible to estimate the economic and organisational requirements mentioned in the second step unless a prognostics framework is established for the system. Altering this step by taking the organizational and economic factors to the last stage could make the process more beneficial. The procedure lacks the required details to ensure that components selected are feasible as there is less importance on failure model selection.

Potential showstoppers in technical feasibility	
t1a	Failure cannot be detected with existing technology
t1b	Failure cannot be predicted with existing technology
t2a	Failure cannot be detected with additional research
t2b	Failure cannot be predicted with additional research

Table 2 Potential showstoppers in technical feasibility

2.2.3. Discussion

1. The reason for the lack of justification for the selected failure models could be that they have concentrated on the system level. It is quite difficult to know all failure mechanisms and failure models as there are no previous studies on guiding towards failure model selection in PoF prognostics.
2. The methods do not specify which categories of models are applicable for old components and new components, respectively. In addition to that, there is no mention of feasible conditions for models (Example – Directionality of stresses in fatigue failure). In both of the methods, no importance has been given to cumulative damage summation models other than LDR.
3. Despite the potential advantage of CDM models, they are not noticed in prognostics literature. Similarly, no importance has been given to cumulative damage summation models other than LDR.
4. To identify the feasible models, a study on matching the variables in the models to the possibilities of sensors is required. This is because, currently, there is no validation on RUL estimation is noticed for the selected models.

2.2.4. Proposed approach to bridge the gap between failure models and Prognostics

A flowchart could be developed to aid in selecting the failure models depending upon the life cycle scenarios and feasible conditions. However, developing only a flowchart and giving an example would not make users aware of the other models. A repository of models is required to make users know the other available models. As feasible conditions may vary among the failure mechanisms, an additional linking tool is required for each failure mechanism to guide in identifying models for respective feasible conditions. Therefore, developing a tool that comprises a flowchart, a repository of models and a linking part between the flowchart and the repository is considered to be a solution to bridge the gap between failure models and prognostics.

Chapter 3. Development of feasibility tool

The feasibility tool has three parts, a database, a guidance sheet, and a flowchart. The database contains the failure models and the parameters used in each of the models. The guidance sheet aids to know which models in the database are feasible for the selected component, failure mechanisms, feasible conditions and available sensors. The flowchart aids to know which category of models in the guidance sheet should be considered based on the life cycle scenarios and certain predefined questions. Therefore, a user can use the flowchart and the guidance sheet to search for a failure model in the database. If the user can install the required sensors and collect the material properties mentioned in those models, PoF prognostics is feasible. If the user is unable to install any of the required sensors or unable to collect the material properties mentioned in the feasible models, then the user can go back to the flowchart to check further possibilities and determine the feasibility.

A new nomenclature for the failure models is used in the feasibility tool. The nomenclature is explained in **section 3.1**. The database, the guidance sheet and the flowchart are discussed in **sections 3.2, 3.3** and **3.4**, respectively. A step by step working procedure of the tool is explained in **section 3.5**. This chapter acts as architecture for the feasibility tool and the tool has been customised for a shaft in the next chapter.

3.1. Nomenclature of failure models

The new terminologies used for grouping the models are tabulated **table 3** along with the explanation of each of the terminologies, an example for each of the terminologies and the respective acronyms. In addition to the acronyms mentioned in the **table 3**, “**FM**” is used as an acronym for failure mechanism.

The terminology	Acronym	Definition	Example
Cumulative Life models	CL	These models calculate the number of cycles/time to failure for a given input value of the load or a manifestation of load in the material. These models require a damage estimator to calculate RUL.	SN curve
Damage Estimators	DE	These models calculate the accumulated damage due to varying amplitude loadings. These models require loading history.	LDR
Condition-based models	CB	These models calculate the number of cycles/time to failure for a given input value of the load or a manifestation of load in the material and a variable that indicates the condition of the material. These models do not require damage estimator to calculate RUL. In addition to that, these models do not require loading history.	Crack growth models
Final Threshold	FT	These are the final limits of the observable effect of the failure mechanisms used in the condition based models.	Critical crack length
Damage Criterion	DC	These models do not calculate the number of cycles/time to fail but check if the material is expected to fail or not due to the input loads	Matake criterion

Table 3 Nomenclature of models

The reason to rename cumulative damage summation models as damage estimators is to avoid confusion with the linear damage summation model and ductility expansion model in TMF. The linear damage summation model and ductility expansion model are cumulative life models.

For constant amplitude loading applications, the cumulative life models do not require a damage estimator to estimate the RUL. However, prognostics is not required for the constant amplitude loadings, according to the author. This is because there is no requirement to monitor a parameter if none of the parameters is going to vary during the operation.

3.2. Database

The current database is presented in **Appendix A**. The database is made up of tables. Each table in the database corresponds to the category of a model mentioned in **table 3** for a specific failure mechanism. For example, table **FM1CL** corresponds to cumulative life models of failure mechanism 1. The first column in each table of the database represents the parameters used in the models. For example, the first column of table **FM1CL** contains the parameters used in the cumulative life models of failure mechanism 1. The parameters are divided into variables and constants. In addition to the parameters used in the models, the feasible conditions of respective failure mechanisms and additional notes are also included in each table if available.

Each model is given identification with the category of the model as the prefix. For example, **CL1** indicates cumulative life model 1. Each model is allotted with a column, and the parameters used in the respective model are indicated with “x” in the cell. Reference for each of the models is provided in the last table of the database, which has been titled **References**. The reference table consists of the model number, category of the model, failure mechanism, literature source, year and the authors.

In the current database, SN curves for corrosion fatigue and crack growth models of TMF have not been included. This is because, SN curves in corrosion fatigue do not take time into account, which is the main factor in the crack initiation period. Crack growth models in TMF are not included due to the complexity involved and limited materials tested. All the other discussed models in **section 2.1** are added in the database. However, it should be noted that the models in the current database are up to the works of the author. There might be some models missed out by the author.

3.3. Guidance sheet

The guidance sheet acts as the link between the database and the flowchart. The guidance sheet indicates the lists of feasible models for the selected failure mechanism, feasible conditions and a sensor. However, the sensors could vary for the same variable in a different component. Hence, for every failure mechanism, there is an ideal guidance sheet which has no mention of sensors but indicates the feasible models for a selected failure mechanism and respective feasible conditions. The ideal guidance sheet is then customised to a specific component of interest, based on the modality of the sensors used for the respective component. Modality refers to the deliverables derived from the output of the sensor. The ideal guidance sheets for each of the failure mechanisms discussed in **section 2.1** has been provided in **Appendix B**. A customised guidance sheet for a shaft is provided in the next chapter. One more reason to have an ideal guidance sheet is that it could reduce time consumption if the same failure mechanism is repeated in another component.

3.4. Flowchart

The flowchart acts as a guide to use the guidance sheet and make final decisions on feasibility. It contains the category of models discussed in **section 3.1** arranged systematically to aid in identifying the specific category of models based on life cycle scenarios and certain predefined questions. There

are two life cycle scenarios (new component, old component) and two ways of RUL estimation (cumulative life models + damage estimators, condition-based models).

For the new components, both condition-based models and cumulative life models are applicable. However, priority is given to cumulative life models. This decision is made based on the possibilities of both the category of models in fatigue failure. In fatigue failure, the cumulative life models calculate the life until crack initiation, and the condition based models calculate the life from crack initiation to the final fracture. In applications where vibration is not favourable, cracks are not preferred as they could increase the vibration levels and lead to loss of accuracy or noise. Therefore, priority is given to cumulative life models as they calculate the crack initiation life. As damage estimators are required for the cumulative life models to estimate the RUL, they are added to the flow, and the flow for the new components is depicted on the left side of **figure 14**. For the old components, condition-based models are only applicable. However, if the old component is operated under loads such that they are still below the threshold limits for failure to occur, it is equivalent to a new component. Therefore a damage criterion could be used to check the possibility of failure to occur. Considering the damage criteria, the flow for the old components is depicted on the right side of **figure 14**.

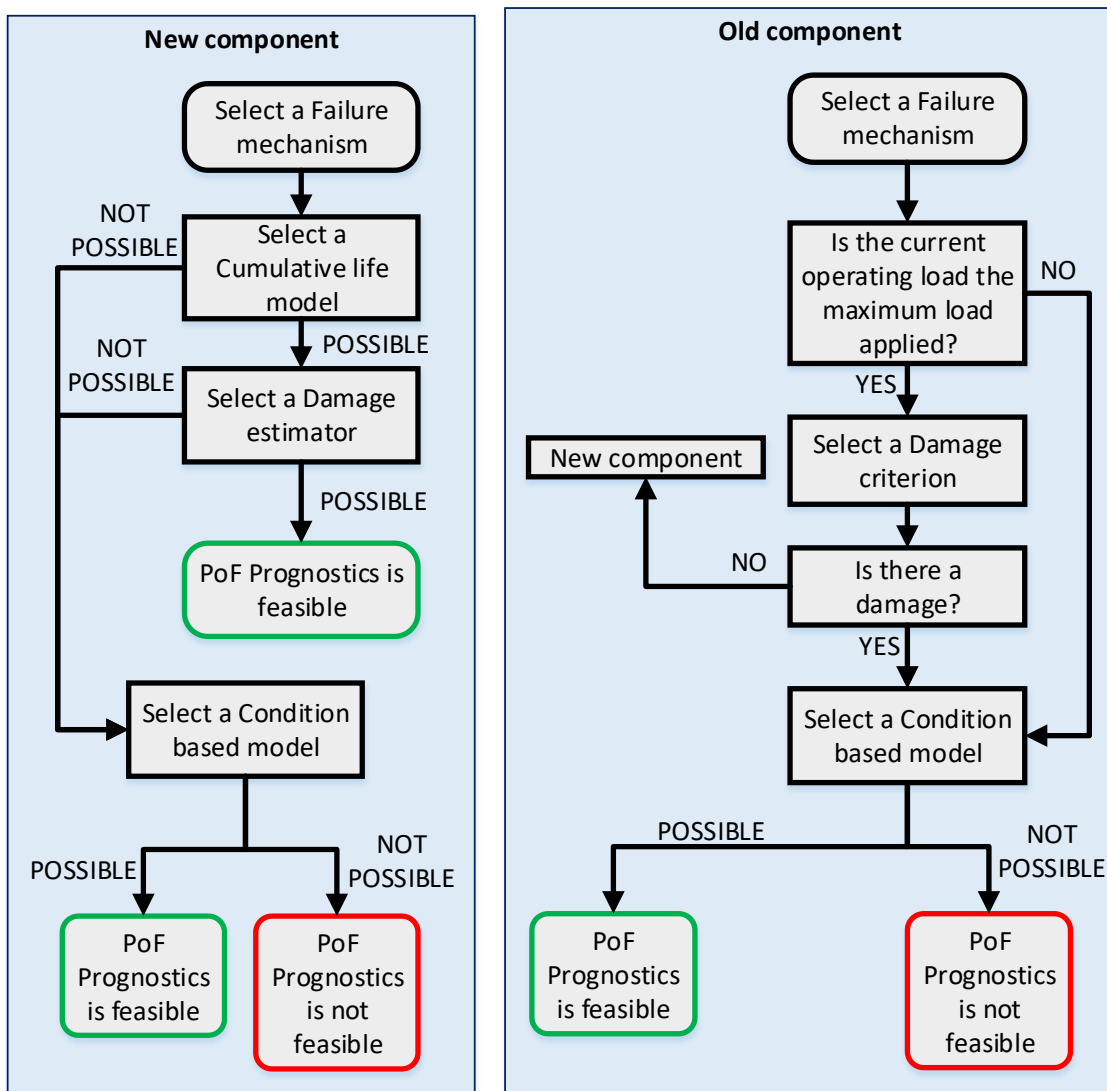


Figure 14 Flow methodology (Left-New component, Right-Old component)

For both the old and the new components, the condition based models are at the last stage. Therefore the last stage is merged. In addition to that, the first step of selecting the failure mechanism is merged. This merging results in the flow as depicted in **figure 15**.

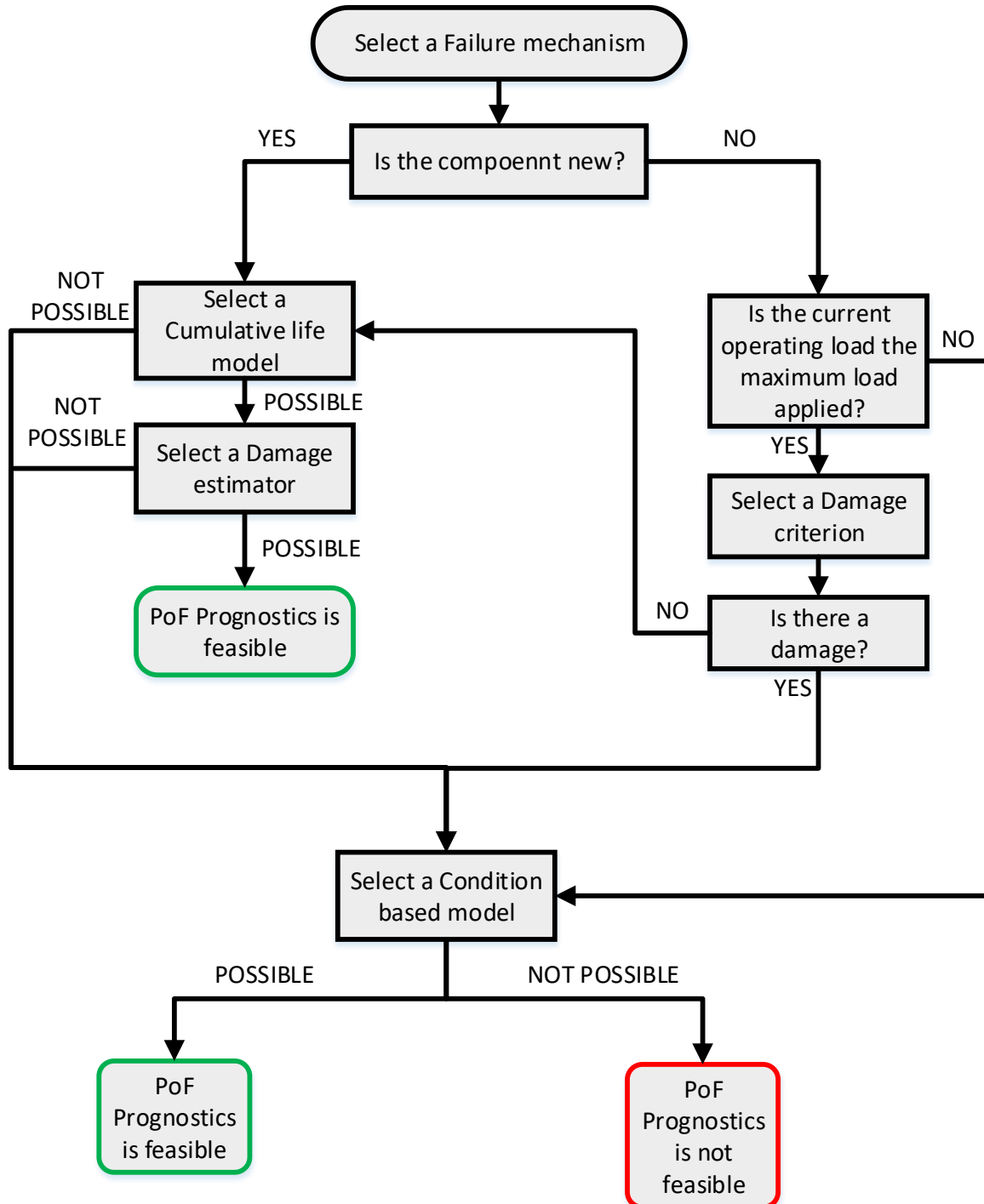


Figure 15 Combined flow methodology for new and old components

In case a user is able to monitor the variable used in the condition based models that correspond to the condition of the component but unable to find the material properties used in that model, trending could be used to estimate RUL. For this purpose, the final threshold of the same variable in the condition based models can be utilised. An example situation where trending could be used: The

user can monitor the dimensions of crack and the stress in the component, able to collect the toughness of the material and geometrical factors for the type of the crack but unable to find the crack growth plot. Therefore, the final threshold is added to the flowchart as the last step.

To make the user aware of redirecting towards the guidance sheet at necessary steps, the outline of the box is differentiated, and a note has been included at the top of the flowchart. The finalised flow is depicted in **figure 16**.

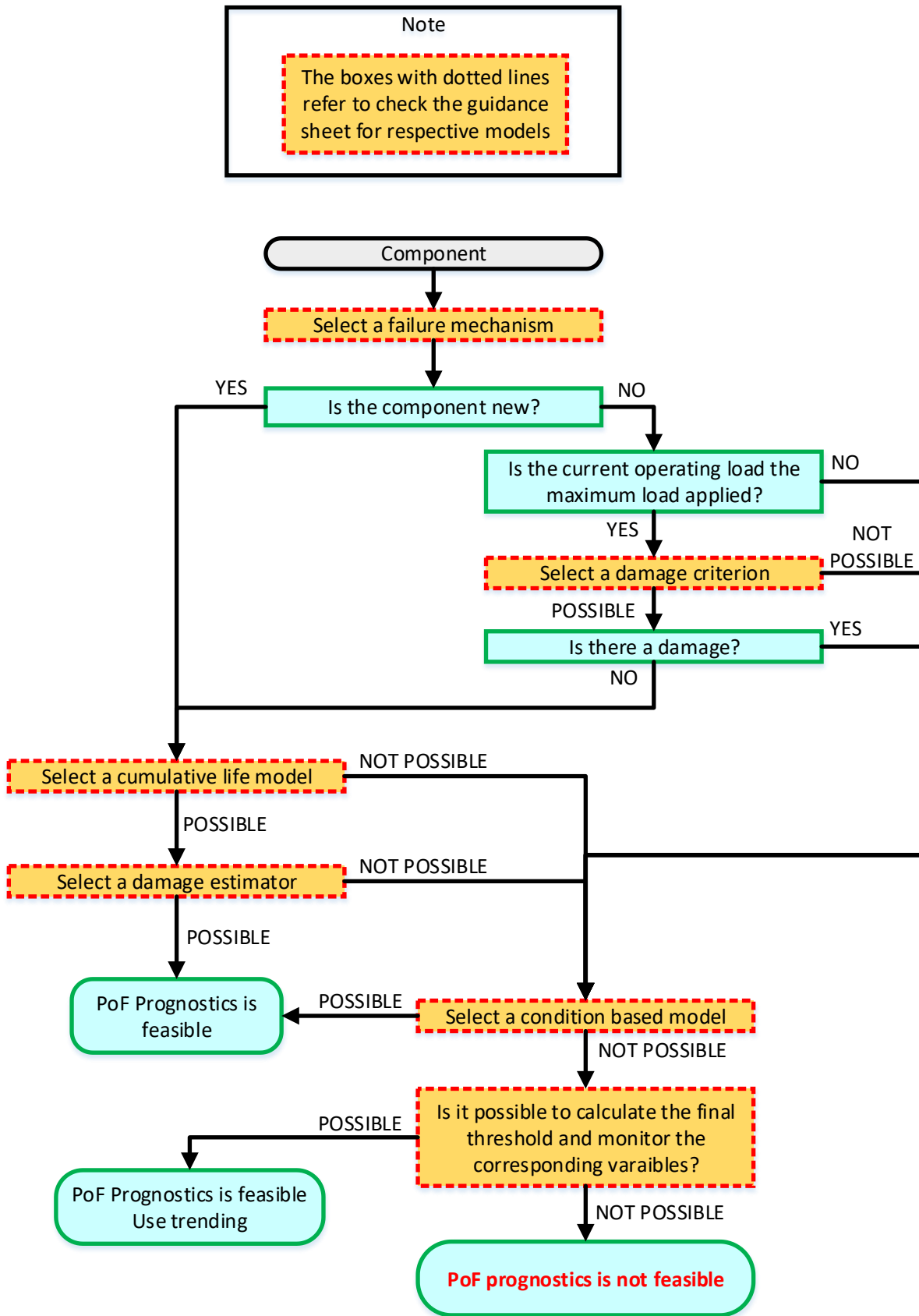


Figure 16 Feasibility flowchart

3.5. Working of feasibility tool

A step-by-step working procedure of the feasibility tool is explained in **table 4** and is also depicted in **figure 17**.

Step	Location	Action
1	Guidance sheet	Selecting a failure mechanism.
2	Flowchart	Selecting the life cycle scenario of the component and answering any question if applicable. Based on that, the flowchart will indicate the category of the model to be checked in the guidance sheet.
3	Guidance sheet	Selecting the feasible condition and respective sensors for the feasible condition. Based on that, the guidance sheet will indicate the feasible models to be checked in the database.
4	Database	Selecting a model depending on the availability of the constants used in the feasible models.
5	Flowchart	If it is possible/not possible to collect the constants for any of the indicated models in the database, then the flowchart will indicate the final decision on feasibility. This has to be repeated until a final decision on PoF prognostics feasibility is made.
Example for Step 5		For a new component, if it is possible to collect the constants for any of the indicated models in the database, then the flowchart will redirect to select a damage estimator. If it is not possible to collect the constants for any of the models indicated in the database, then the flowchart will redirect to select a condition-based model.

Table 4 Step-by-step working procedure of the feasible tool

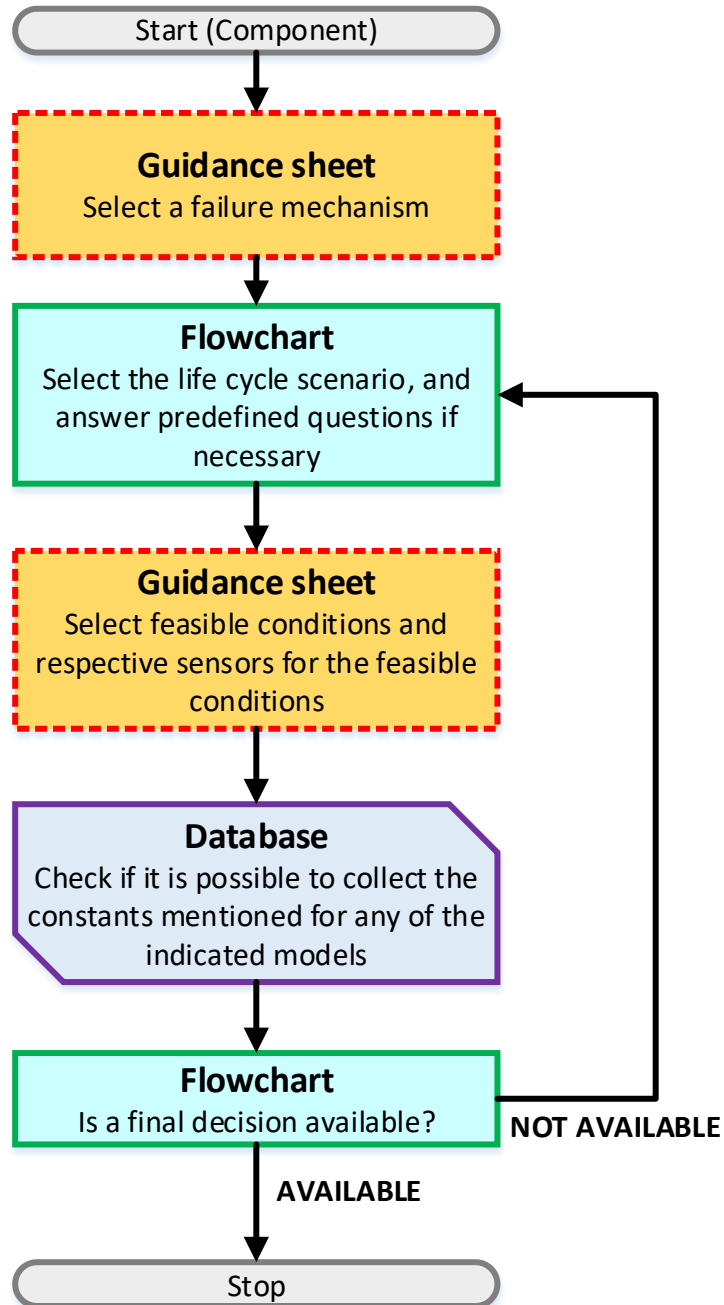


Figure 17 Working of the feasibility tool

Chapter 4. Demonstration of the feasibility tool

To demonstrate the feasibility tool for a component, a study on the sensors used for the component and the failure models of associated failure mechanisms of the component is required. For demonstration, a shaft is chosen as the cases study component. The failure mechanisms associated with a shaft and the associated failure models have already been discussed in chapter 2. However, the failure models required only for the loading conditions of a shaft has to be identified. These models are termed as possible models. The variables used in those possible models are simplified to the basic form so that it could help in checking against the modality of the available sensors, and aid in identifying the feasible models. This process of identifying the feasible models is discussed in **section 4.1**. Based on the feasible models, the feasibility tool for a shaft is customised in **section 4.2**. Besides the customisation, the tool has been used in **section 4.3** to find feasible models for two real-time applications. This is followed by a discussion on misunderstanding in shaft design in **section 4.4**.

4.1. Feasible models for a shaft

4.1.1. Possible models

The feasible conditions for the failure mechanisms of a shaft are the directionality of stresses and the material. These feasible conditions are applicable for cumulative life models, condition-based models and damage criterions.

Cumulative life models, condition-based models and damage criterions

The directionality of stresses depends on the loading. A shaft could have bending, torsion or a combination of bending and torsion. These configurations and their corresponding directionality of stress are tabulated in **table 5** along with an example.

Configuration	Example	Loading scenario
Bending	Non-driven axles of railway bogie	Uniaxial
Torsion	Connecting shafts in industries without any inclination angle in the joints	Shear stress
Combined bending and torsion	Driven axles of railway bogie	Multiaxial non-proportional

Table 5 Loading configurations in a shaft

Among the collected models in the database, there are models for uniaxial conditions and multiaxial non-proportional conditions. There are no models dedicated to pure shear conditions. Therefore the uniaxial models in which the tensile properties could be substituted with the shear properties are selected for torsion loading. Considering the substitution mentioned above, the possible cumulative life models, condition-based models and damage criterions are tabulated in **tables 6, 7 and 8** respectively. FRC in **tables 6, 7 and 8** refers to fibre reinforced composites.

Failure mechanism	Material	Configuration		
		Bending	Torsion	Combined bending and torsion
Fatigue (FM1)	Metals	CL1-CL9	CL1-CL6	CL11-CL23
	FRC	CL1-CL2	CL1-CL2	Not available
TMF (FM3)	Metals	CL1-CL14	CL1-CL11, CL13	CL15
	FRC	Not available	Not available	Not available
Fretting fatigue (FM4)	-NA-	CL1		

Table 6 Possible cumulative life models for a shaft

Failure mechanism	Material	Configuration		
		Bending	Torsion	Combined bending and torsion
Fatigue (FM1)	Metals	CB1-CB11	CB1-CB11	CB12-CB13
	FRC	CB1	Not available	Not available
Corrosion fatigue (FM2)	Metals	CB1-CB6	CB1-CB6	Not available
	FRC	Not available	Not available	Not available

Table 7 Possible condition-based models for a shaft

Failure mechanism	Material	Configuration		
		Bending	Torsion	Combined bending and torsion
Fatigue (FM1)	Metals	DC22	DC22	DC2-DC21
	FRC	DC22	DC22	Not available

Table 8 Possible damage criterions for a shaft

Damage estimators

The feasible conditions for the damage estimators are the material and the inclusion of the effect of load sequence. Variable amplitude loading causes the load sequence effect by default. However, all the damage estimators are analysed because; the estimators that do not take load sequence effect into account are the most widely used.

4.1.2. Shaft sensors

The sensors that are currently used for shafts are presented in **table 9**, along with their primary deliverable [66]–[71]. The possibilities of each of the deliverable from the respective sensors are depicted in **figure 18**. Material data such as the elastic modulus, shear modulus, and the dimensions of the shaft are required for the final outputs (represented in blue boxes) in **figure 18**. The process of deriving the variables from the respective sensors is explained as follows.

Measurement	Sensor/technique	Measurement	Sensor/technique
Strains	Strain gauge rosette	Vibration	Eddy current sensors
	Strain gauge rosette		Ultrasonic sensors
Torque	Inline torque cell		Optical grating sensors
	Clamp-on torque cell		Accelerometers
	Dual range torque sensor		Temperature
	Surface acoustic wave torque cell	Thermocouples	
	Inductive encoders		
	Optical grating sensors		

Table 9 Shaft sensors

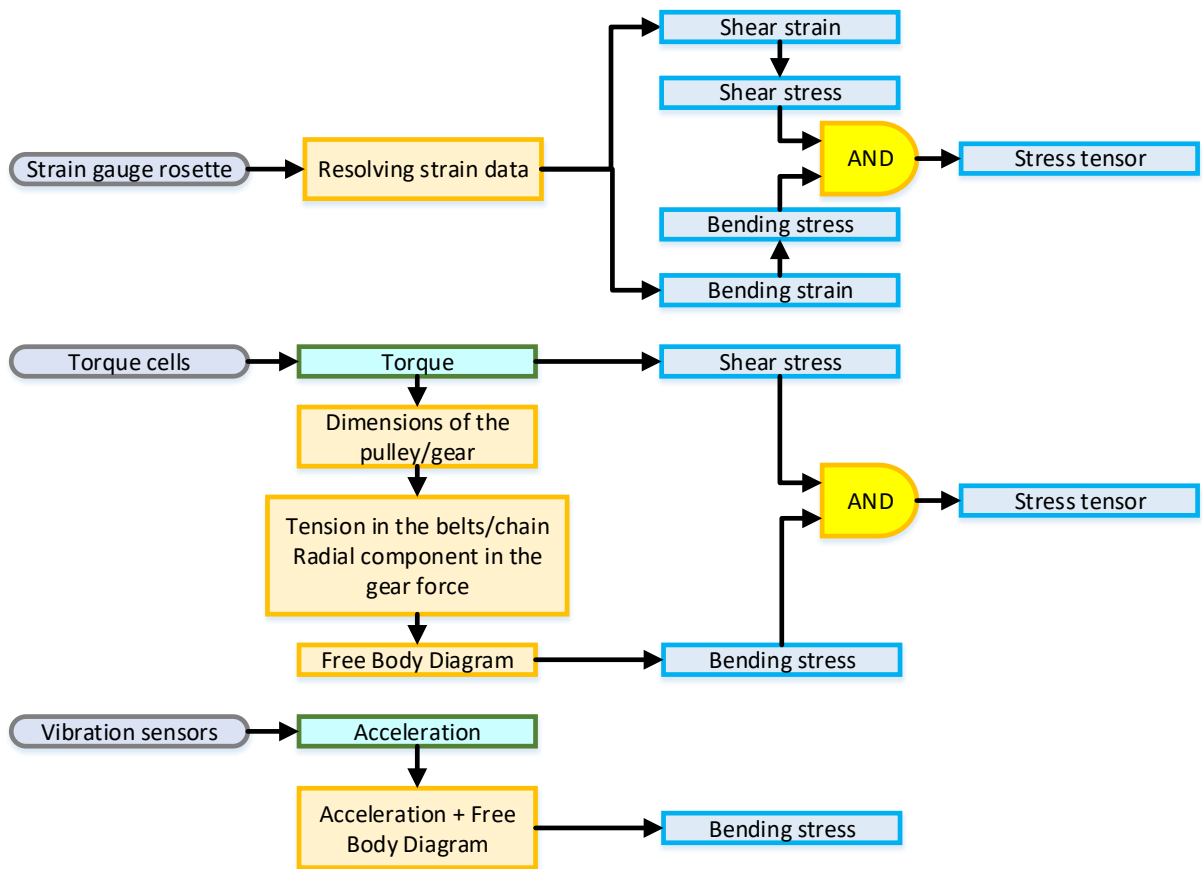


Figure 18 Deliverables of the shaft sensors

i. Strain gauge rosette

The strain measurement obtained from the strain gauge rosettes could be used directly in the models or could be converted to the respective stress forms. However, strain gauges do not give the shear strain or bending strain directly. They are installed in rosettes, and the strain data from different orientations have to be resolved to obtain shear and bending strains. Bending and shear stresses are calculated from respective strains. As both bending and shear stresses are available, strain gauge rosettes could be used to build a stress tensor. The axes representation of the stress components of a shaft subjected to combined bending and torsion is depicted in **figure 18**, and the corresponding stress tensor is mentioned in **equation 23**.

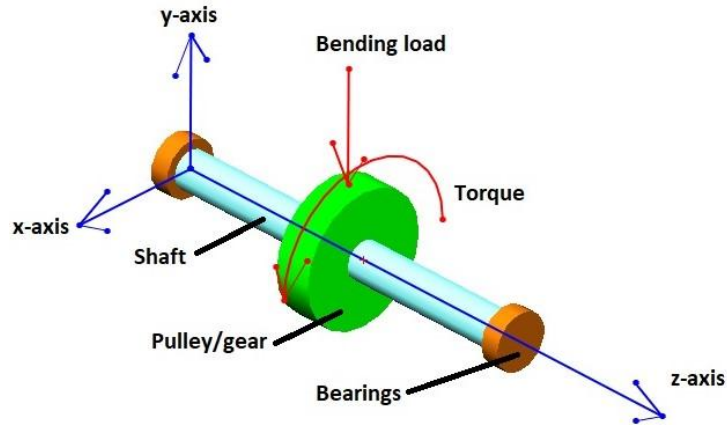


Figure 19 Axes representation for stress tensor in a shaft

$$\sigma = \begin{bmatrix} 0 & 0 & \tau_{xz} \\ 0 & 0 & \tau_{yz} \\ \tau_{zx} & \tau_{zy} & \sigma_{zz} \end{bmatrix} = \begin{bmatrix} 0 & 0 & \tau \\ 0 & 0 & \tau \\ \tau & \tau & \sigma \end{bmatrix} \quad (23)$$

ii. Torque cells

Torque cells produce torque as their output. Shear stress could be calculated from the torque. Torque cells cannot calculate bending stress directly. However, torque can be used to calculate the tension in the belts/chains and radial force component in gears. Bending stress in a shaft can be calculated from tension in the belts/chains and radial force components. In this manner, a torque cell can be used to obtain bending stress, and form a stress tensor in combination with the shear stress.

iii. Vibration sensors

In addition to the torque cells and strain gauges, the acceleration data obtained from the vibration sensors can be used to calculate bending stress in a shaft[72]. Unlike torque cells/strain gauge rosettes, the mass of the shaft is required for stress calculation in combination with acceleration data.

4.1.3. Feasible models

To identify the feasible models, the variables used in the possible models have to be cross-checked with the final outputs of sensors mentioned in previous **subsection 4.1.2**. The variables used in the possible models are simplified to their manifestation in a shaft. For example, stress amplitude refers to bending stress in a shaft; similarly, octahedral shear stress requires stress tensor, and a stress tensor for a shaft requires bending stress and shear stress in the shaft. This simplification and matching against the final outputs are tabulated in **Appendix C**.

However, some variables which cannot be manifested in a shaft/requires FE tool/requires laboratory level setups/do not have sensors are tabulated in **table 10**. The rest of the variables are matched with the sensors resulting in feasible models as tabulated in **Table 11**. **Table 11** is the guidance sheet for a shaft. In **table 11**, there is a column titled "without sensor". This column contains the models where the parameters are calculated from another model type or by counting (example – variables used in LDR do not require any sensor).

Variables	Reason for non-feasibility
Normal strain excursion between two turning points of shear strain	FE tools required
Stresses and strains acting on a particular plane	FE tools required
Resolved shear stress	FE tools required
Location and angle between the planes	FE tools required
Drag stress	FE tools required
Volume and strain energy volumetric density at critical points	FE tools required
Friction stress	Not required for shaft
Strain partitioning variables in TMF models	Lab level controlled setup
Cyclic hardening rate	Lab level controlled setup
Surface layer stress	Lab level controlled setup
Nucleation strain	Lab level controlled setup
Coalescence strain	Lab level controlled setup
Crack/Pit dimensions	No sensor available for continuous monitoring during operation

Table 10 Variables that could not be derived from the available sensors

Model	Failure mechanism	Configuration	Strain gauge rosettes	Torque cells	Vibration sensors	Temperature sensors	Without sensor
Cumulative life model (CL)	Fatigue (FM1)	Bending	CL1-CL9		CL1, CL2, CL7, CL9		
		Torsion	CL1-CL9	CL1, CL2, CL7, CL9			
		Combined bending and torsion	CL11-CL13, CL15-CL19, CL22-CL23	CL12, CL22, CL23			
	TMF (FM3)	Bending	CL1-CL11, CL13			CL1-CL7	
		Torsion	CL1-CL11, CL13			CL1-CL7	
Damage estimator (DE)	Fatigue (FM1)	Not applicable	DE2, DE7-DE10, DE13-DE15	DE3-DE7, DE14-DE15	DE3-DE7, DE14-DE15		DE1, DE3-DE6
	TMF (FM3)		DE2-DE6	DE2	DE2		DE1
Damage criteria (DC)	Fatigue (FM1)	Bending	DC22		DC22		
		Torsion	DC22	DC22			
		Combined bending and torsion	DC2-DC11, DC17-DC19, DC21	DC2-DC11, DC18-DC19, DC21			

Table 11 Guidance sheet for a shaft

4.1.4. Reasons for non-feasibility of other mechanisms

i. Non-feasibility of condition-based models

As all the condition based models in the failure mechanisms associated with the shaft have dimension as one of the parameters, and there are no sensors currently available for monitoring the cracks continuously, all of the conditions based models become non-feasible.

ii. Non-feasibility of combined bending and torsion in TMF

Only one model (FM3CL15) from TMF is capable of handling non-proportional stress. In this model, the variable “drag stress” cannot be obtained through the available sensors. Therefore this model is not feasible for prognostics.

iii. Non-feasibility of Corrosion fatigue

Only condition-based models are available for corrosion fatigue as corrosion fatigue SN curves were excluded from the database, as explained in **section 3.2**. All the condition based models of corrosion fatigue are non-feasible as there are no sensors available to monitor the cracks continuously.

iv. Non-feasibility of Fretting fatigue

Only one model has been found for fretting fatigue. This model uses localised shear stress which requires FE tools or a lab level arrangement to calculate the localised stress.

4.2. Customisation of feasibility tool for a shaft

1. Guidance sheet - The guidance sheet for a shaft has already been tabulated in **table 11**. Changes include substituting loading configurations instead of the directionality of stresses.
2. Flowchart - The flowchart need not be customised. However, customisation of the flowchart is up to the preferences of a developer. Similar to the guidance sheet, the loading configurations are included in the flowchart instead of the directionality of stresses. In addition to that, shaft failure mechanisms and the sensors for respective configurations are also added to the flowchart. The resultant customised flowchart is depicted in **figure 20**.

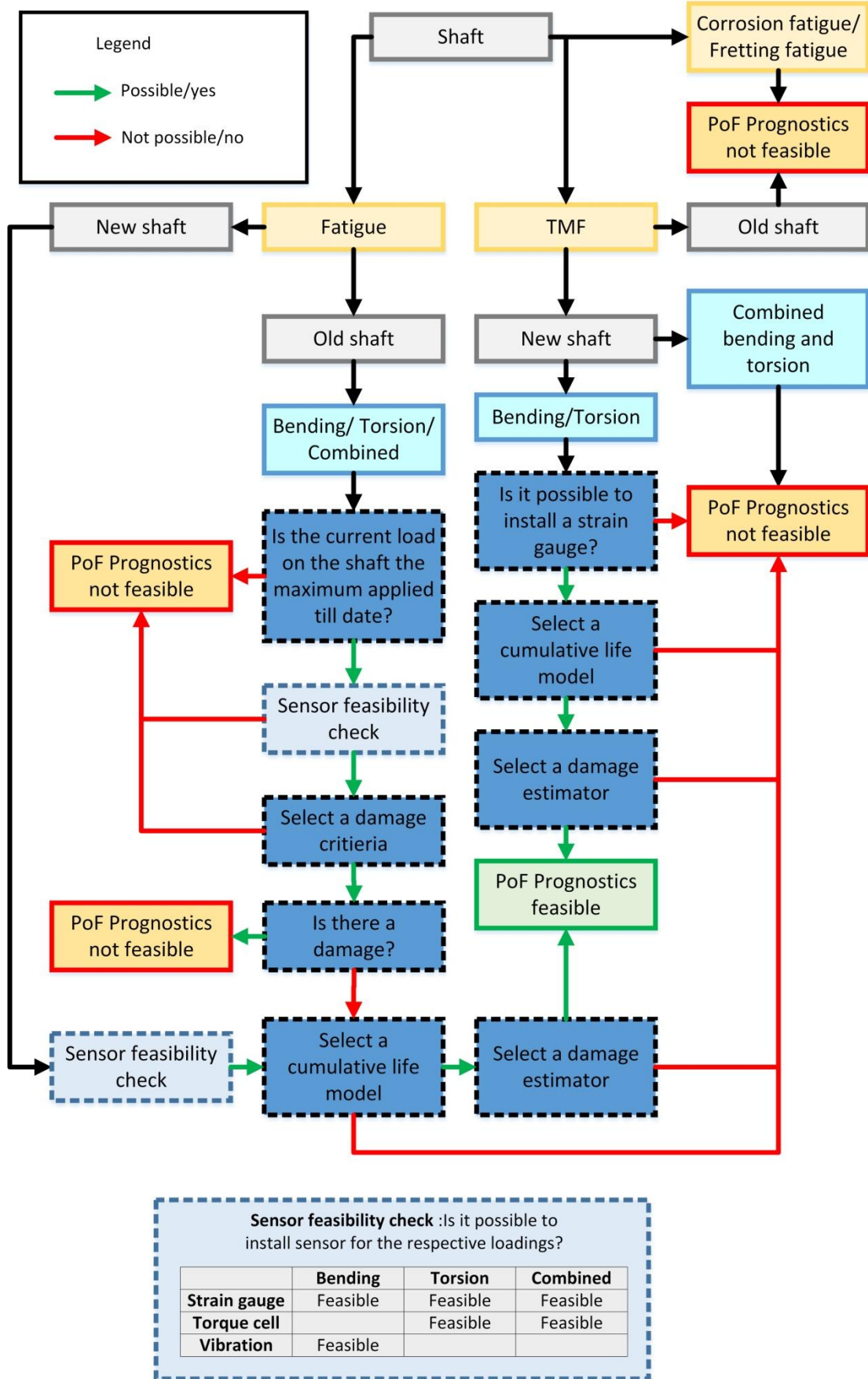


Figure 20 Customised feasibility flowchart for shaft

The current customised flowchart in **figure 20** does not indicate the reasons for non-feasibility. The non-feasibility has been determined by the author in terms of non-availability of a sensor to monitor a variable or non-availability of a model. However, a user might have a solution to monitor that variable or propose a new failure model. Therefore, the flowchart and the guidance sheet are customised further and represented in **Appendix D**.

4.3. Case studies

In addition to the customisation of the feasible tool, it is used to find feasible models for two real-time applications. They are

1. Spinner separator shaft - The customised feasibility tool for a shaft is used for the spinner separator shaft. Feasible models are identified for both old and new shafts.
2. Composite beam tested in SLOWIND Project - For the composite beam, the ideal guidance sheet and the database are only used. This is because; the composite beam has already been tested, and feasible models are identified for the collected dataset. Therefore, the second case study aids in knowing the importance of the ideal guidance sheet.

4.3.1. Spinner separator shaft

A spinner separator is a rotating filter that is used to separate the ground particles based on its size. Spinner separators are used extensively in grinding and drying applications in coal and ore industry. A typical setup of a spinner separator assembly is depicted in **figure 21**. The setup consists of a vertically mounted cylindrical main body shell which has the spinner separator at the top and the grinding assembly at the bottom. Hammers do grinding. Drying is achieved by blowing hot compressed air from the bottom, and the compressed air also acts as a transport medium to transport the particles from the ground to the top. The temperature of the compressed air varies from 140 – 400 degree Celsius depending on the coal/ore used [73].

A spinner separator assembly consists of spinning blades attached to a shaft that is driven by an external source. In the application chosen for the case study, it is driven by an external electric motor attached to the shaft via a belt. The shaft is made up of mild steel. While the spinner separator is rotating, the ground particles those are small enough to pass through the gap between spinner blades while the larger particles fall back to the grinder. The filter size is varied by altering the speed of the spinner. To isolate the vibration resulted from the grinding process; a rubber expansion joint is mounted in the channel between the grinding assembly and the spinner separator assembly.

Feasible model identification

1. The initial step in the feasibility tool is to select the failure mechanism. As the maximum operating temperature is 400 degree Celsius which is still below 35% of the melting temperature of the mild steel (525 degree Celsius), TMF is not considered [74]. This is because; TMF is a combination of fatigue and creep. Creep occurs above 35% of the melting temperature of the material. The reasons for other possible failure mechanisms are explained as follows.
 - Fatigue – Due to cyclic stress in the shaft
 - Corrosion fatigue – Due to moisture. However, PoF prognostics for corrosion fatigue is not feasible, as explained in **subsection 4.1.4**.
 - Fretting fatigue – This can happen accidentally and not due to its design or operation. Fretting might occur in the key slots or in the place of bearing races. In case fretting happens, PoF prognostics is not feasible as explained in **subsection 4.1.4**.

Therefore, feasible models are identified for fatigue failure.

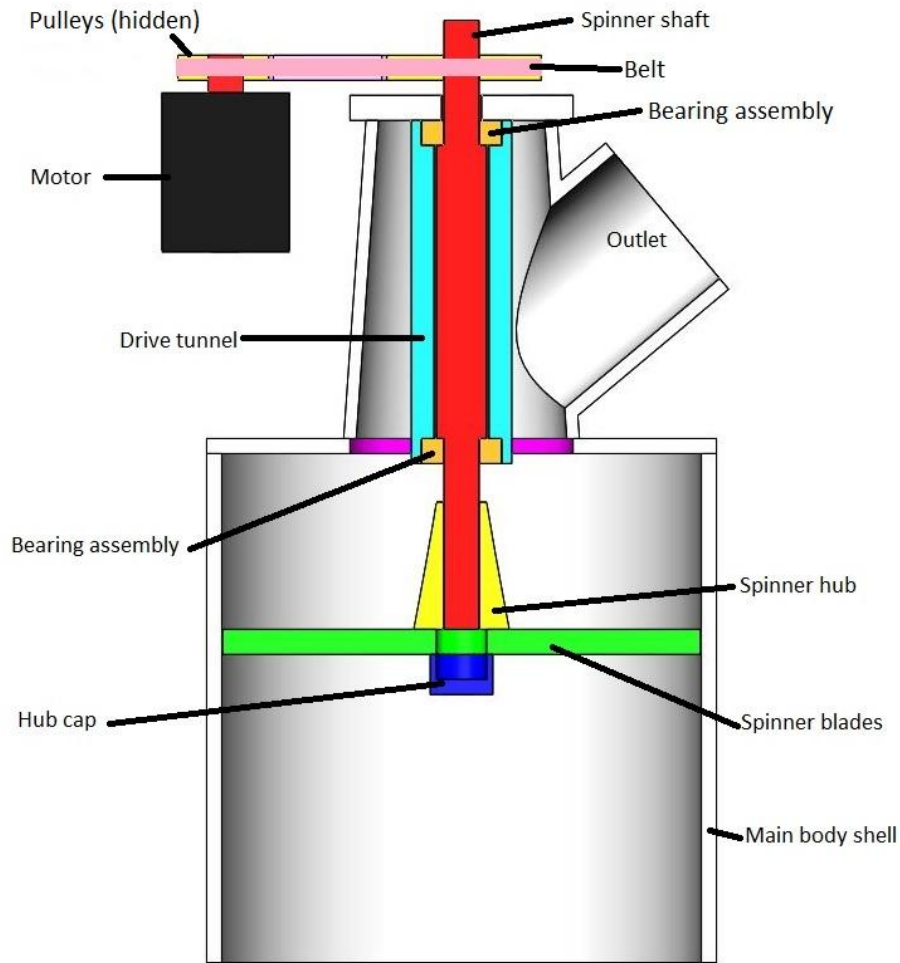


Figure 21 Spinner separator assembly

2. The next step is to select the life cycle scenario. Feasible models are identified for both old and new shafts. PoF prognostics is not feasible for an old and damaged shaft as all there are no sensors to utilise the condition based models.
3. The next step is to identify feasible conditions. The feasible conditions are material, the directionality of stresses and sensors. The material used is mild steel, which is a metal. Due to a pulley attached and torsional load, the stresses are multiaxial non-proportional. For this stress, strain gauge rosettes and torque cells are applicable. There is no possibility to mount any of those sensors inside the drying chamber in the gap between the spinner hub and bearing isolator because of the operating environment. This is because; the ground particles could get deposited on the receivers of the sensors. Therefore, the possibilities for mounting them outside are checked. As the sensors would give zero readings on the free ends of the shaft, the sensors have to be mounted between the pulleys and the casing. There are two options.
 - i. If an extension of the spinner shaft is permitted, strain gauges could be installed between the hub and the bearing assembly on the exterior side of the main body.
 - ii. In case the shaft could not be extended, the electric motor has to be lowered, and adapters could be made for a readymade torque cell to be mounted with the pulley and the shaft of the electric motor as shown in **figure 22**.

Among the two strategies, the second strategy is chosen due to the lesser number of steps involved in the installation.

4. Feasible models (Models are obtained from the guidance sheet customised for a shaft)
 - i. Cumulative life models – CL12, CL22 and CL23.
 - ii. Damage estimators – DE3-DE7, DE14-DE15
 - iii. Damage criteria- DC2-DC11, DC18-DC19, DC21

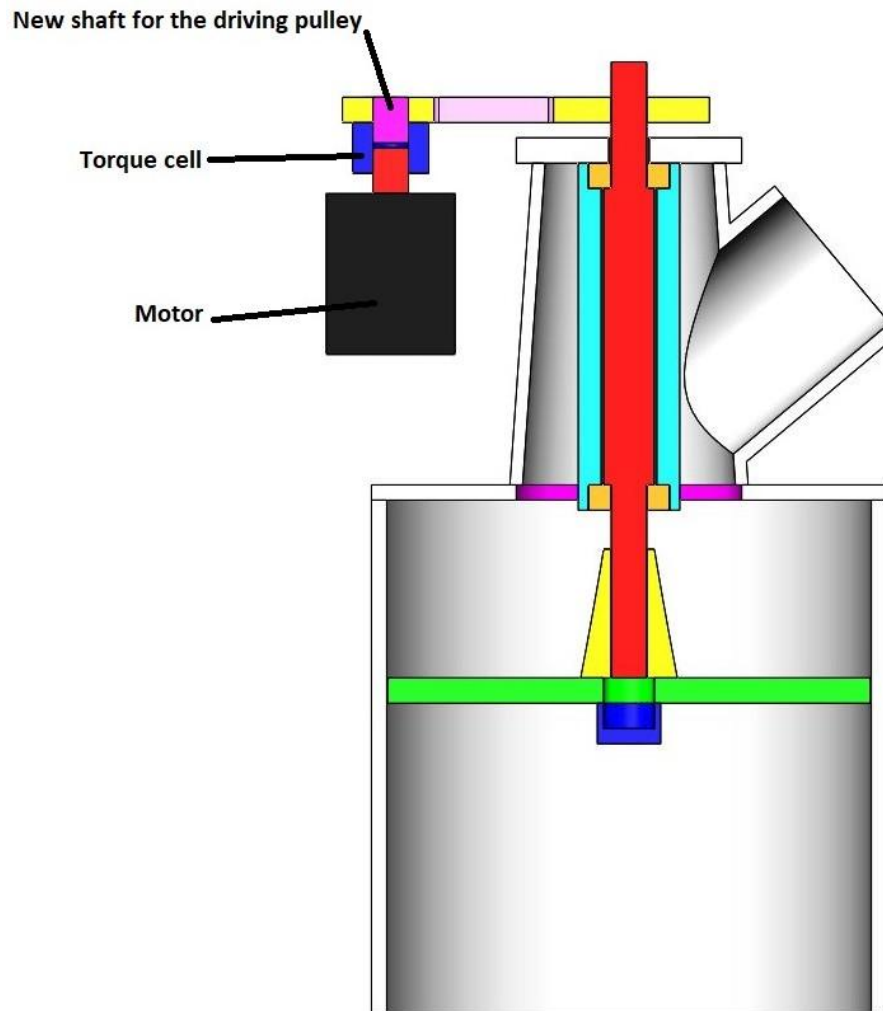


Figure 22 Suitable position for torque cell

4.3.2. Composite beam tested in SLOWIND project

A fatigue testing has been conducted in the composite beam using a three-point bending setup [75]. Feasible models have to be identified for the collected data during the fatigue test. As the feasibility tool is customised for a shaft, the ideal guidance sheet is used. The feasible conditions for fatigue failure are material and directionality of stresses. As the material used here is a fibre reinforced composite, only the empirical models such as the SN curves and Paris crack growth law are possible to be checked. The three-point bending setup results in uniaxial stress and both the models (SN curves and Paris crack growth law) apply to this loading configuration.

1. SN curve - The only variable in the SN curve is the stress amplitude. As the test involved the measurement of force as one of the parameters, the bending stress in the beam could be calculated from the force applied. Since fatigue testing has been done under constant amplitude, there is no requirement of damage estimator.

2. Crack growth model (Paris law) – The variables required for the crack growth model are the crack dimensions and the stress concentration factor. The stress concentration factor could be calculated from the stress amplitude (stress amplitude calculation is done as mentioned previously through the force signal). The crack dimensions during the test have not been measured. However, the damage accumulation plot from the ultrasonics sensors shows a sudden rise at the end of the experiment. The beginning of the spike could be assumed as the crack growth initiation life, and the remaining cycles could be checked with crack growth model iteratively assuming different crack lengths.

4.4. Misunderstanding in shaft design

In PoF prognostics of a shaft, only one study has been found which is a laboratory experiment comparing the time domain models and frequency domain models [72]. As this experiment has been conducted on uniaxial bending case, there is no literature available for combined bending and torsion configurations. Therefore literature on designing of shafts and failure investigation of shafts were considered. Two design codes are widely used in designing of shafts. They are ASME B106.1M:1985 and DIN 743 [76]. Both of the design codes use only octahedral shear stress which does not take non-proportionality into account [24][77].

This misunderstanding of non-proportional stress is not noticed in automotive literature but only in machinery shafts[78]–[80]. The only exception is a study on failure analysis of a driven axle of a train [81]. In this study, non-proportionality is not considered. The railway axles are subjected to variable loading as it depends on the payloads (passengers and cargo). In the study, it has been analysed with a constant loading rather than variable amplitude loading which indicates that the importance of load sequence effect is not considered.

Chapter 5. Discussion, Conclusion and Recommendations

5.1. Discussion on research questions

i. What are the failure models available in literature?

Due to the sheer volume of failure models, the models associated with the failure mechanisms of a shaft have been analysed. The failure models are compiled in **figure 5**, and among the failure mechanisms identified in **section 2.1**, the literature and the number of failure models available for pure fatigue are higher than the synergetic failure mechanisms of fatigue. There are many models for multiaxial non-proportional loadings in pure fatigue compared to TMF. No models are found in corrosion fatigue and fretting fatigue for non-proportional loadings. Among the literature on fatigue models, the number of damage criteria is higher than cumulative life models. Damage estimators are only available for pure fatigue, some of which could be used for TMF. There are no damage estimators dedicated to TMF, corrosion fatigue and fretting fatigue. Only one standard model is available for fretting fatigue.

ii. How can the failure models be classified?

The failure models are classified depending on the way they estimate the RUL. They are classified into cumulative life models and condition-based models. In addition to that, the cumulative damage summations theories are renamed as damage estimators to avoid confusions with a similar name in cumulative life model categories of TMF. Cumulative life models are applicable for only new components, but condition-based models are applicable for both old and new components. The damage criteria are used with the same name, and the final critical value of a condition-based model in a failure mechanism is termed as the final threshold.

iii. What are the variables used in the models?

Fatigue - The variables used in the models depend on the directionality of stresses. In uniaxial models, the variables are stress/strain/energy parameters or a derivative of stress/strain/energy. In multiaxial models, the variables are derivative of stress tensor or a combination of strain and normal stresses. In addition to that, crack length is used in crack growth models.

TMF - Majority of the models utilise strain or derivatives of strain as the variable. The other variables include a derivative of stress, frequency of loading, temperature and drag stress.

Corrosion fatigue - Stress amplitude, pit and crack dimensions, friction stress, pitting current and frequency.

Fretting fatigue – Localized shear stress.

iv. What are the monitoring techniques available for those variables?

As the shaft is the case study component, shaft sensors were analysed. The sensors include strain gauge rosettes, torque cells, vibration sensors and temperature sensors. In this research, steps to build a stress tensor using torque cell and strain gauge rosettes have been developed. This is because most of the multiaxial models use derivatives of stress tensor as variables. Based on these feasible models for a shaft were identified by matching against the variables used in the models.

v. How could this collected information on models and monitoring techniques be utilised to develop a tool that could aid in identifying the feasible models?

The classified models are arranged in the flowchart as depicted in **figure 16**, and the same classification is used to store the models in the database as presented in the **Appendix A** and in the

guidance sheet as mentioned in the **Appendix B**. These three parts form together feasibility tool. The procedure given in Chapter 3 acts architecture and could be customised for any component.

For a failure mechanism, the PoF prognostics feasibility is determined on the basis that a user is possible to monitor the variables and collect the constants mentioned in the respective feasible models. If the component has already been analysed with the available sensors, then the PoF prognostics feasibility is determined on the basis that user is possible to install the sensors mentioned in the feasibility tool and be able to collect the constants mentioned in the respective feasible models.

As models and sensors for a shaft have been identified, this tool has been customised for a shaft. Based on that, PoF prognostics feasibility has been identified, and the possibilities are tabulated in **table 12**.

Life cycle scenario	New	New	New	New	New
Sensors	Bending	Torsion	Combined bending and torsion	Bending (TMF)	Torsion (TMF)
Strain gauge rosettes	Feasible	Feasible	Feasible	Feasible	Feasible
Torque cells		Feasible	Feasible		
Vibration sensors	Feasible				
Pyrometer/thermocouple				Feasible	Feasible

Table 12 PoF prognostics Possibilities of a shaft (Only for new shaft)

PoF prognostics is not feasible for combined bending and torsion in TMF as one of the variables used in the identified model is not possible to monitor/derive with the available sensors. As there are no sensors currently available to monitor the crack continuously in the shafts, the crack growth models in plain fatigue and corrosion fatigue could not be utilised. Therefore, PoF prognostics is not feasible for old shafts in plain fatigue and both old and new shafts in corrosion fatigue. For fretting fatigue, only one model has been identified which depends on localised shear stress. This parameter requires cannot be derived with the available sensors. Therefore, PoF prognostics is not feasible for fretting fatigue.

5.2. Potential models for fatigue in maintenance

Fatigue models based on the continuum damage mechanics approach are potential for components subjected to variable amplitude loading with multiaxial non-proportional stress. The prime advantage of those models is that the damage estimator and the cumulative life model are derived from a single parent equation. Therefore, they are functions of each other, and it is not necessary to search for a damage estimator separately. This reduces the time consumption in collecting the material parameters if the models are different. In addition to that, CDM models also take the effect of load sequence into account. Despite this advantage over other models, they are not noticed in prognostics literature.

5.3. Conclusion

In this research, failure models of shaft failure mechanisms have been analysed to find the different ways of RUL estimation and applicability of models to the life cycle scenarios. With the help of this analysis, a new nomenclature for failure models has been proposed, and a feasibility tool has also been developed using the new nomenclature. However, the failure mechanisms, models and sensors could vary for other components. Keeping this in mind, the tool has been developed generically that

it could be customised to any component. To demonstrate it, the tool has been customised for a shaft, and feasible models for a shaft have been identified. It has been found that PoF prognostics is feasible for only certain failure mechanisms of the shaft and certain loading configurations. Especially, no monitoring techniques have been identified for the condition based models. This insists that PoF prognostics could only be implemented for shafts that are operated in controlled conditions as the cumulative life models cannot detect or take damage into account. In addition to developing the tool, the literature study on fatigue models aided in revealing the advantages of CDM models.

5.4. Recommendations

i. Extension of the database to other materials

The current database contains models collected for metals except for the classical empirical models. Fatigue modelling of fibre reinforced composites and elastomers are different from those of metals. Extension of the database could also aid in covering more components.

ii. Extension of the database to include material properties

The variables are studied against the possibilities of available sensors. So, the user does not need to know the sensors for selecting a model. However, the user has to look into the database to check if the material properties required for the model can be obtained. The current database only presents the required material properties to run a model and not the material properties. Therefore, the addition of material properties for the available materials would also help in narrowing down the feasibility check. An alternative is also to link to an already available online material database.

iii. Addition of feasibility conditions depending on other factors

The non-proportional loading cases could be divided into synchronous and asynchronous loading. In the current scenario, this classification is rarely addressed. For the shaft, asynchronous loading is never going to happen, because the shear load could be varying but not cyclic and bending load is always cyclic, which makes it less concern for shafts. But in general, adding such advanced classifications along with ductile and brittle materials could make the tool much more accurate in narrowing down the selection of the model.

iv. Conversion of the feasibility tool into a computer application

Currently, the feasibility tool is present in tables and flowcharts with the author as the owner. To avoid confusion and to reduce time in the selection of models, this tool could be made into a computer application. In doing so, a provision has to be made for uploading the models according to the definition of each category of models mentioned. The tool could also be made available online to support other people to upload models. This could update the database and also the tool. Hence, a provision should be made to upload failure models according to the new classification and mark them against components with the available sensors if any.

v. Fully-fledged prognostics tool

Though this tool helps in identifying feasible failure models, it does not help in the identification of failure mechanisms. FAME-X is a failure mechanism identification tool, which gives out the failure mechanisms based on inputs given for a predefined set of questions. On merging this tool with the currently proposed tool, it makes a user select the failure mechanism for his/her working environment. In this way, it makes it easier to identify the failure mechanisms and select a model.

vi. Other recommendations

As CDM models are more advantageous, experiments could be conducted to obtain material properties for commonly used materials.

References

- [1] H. M. Elattar, H. K. Elminir, and A. M. Riad, "Towards online data-driven prognostics system," *Complex Intell. Syst.*, vol. 4, no. 4, pp. 271–282, 2018.
- [2] D. An, N. H. Kim, and J. H. Choi, "Options for prognostics methods: A review of data-driven and physics-based prognostics," *PHM 2013 - Proc. Annu. Conf. Progn. Heal. Manag. Soc. 2013*, pp. 642–655, 2013.
- [3] "RUL Estimation Using RUL Estimator Models - MATLAB & Simulink - MathWorks India." .
- [4] A. Heng, S. Zhang, A. C. C. Tan, and J. Mathew, "Rotating machinery prognostics: State of the art, challenges and opportunities," *Mech. Syst. Signal Process.*, vol. 23, no. 3, pp. 724–739, 2009.
- [5] A. K. S. Jardine, D. Lin, and D. Banjevic, "A review on machinery diagnostics and prognostics implementing condition-based maintenance," *Mech. Syst. Signal Process.*, vol. 20, no. 7, pp. 1483–1510, 2006.
- [6] J. Lee, F. Wu, W. Zhao, M. Ghaffari, L. Liao, and D. Siegel, "Prognostics and health management design for rotary machinery systems - Reviews, methodology and applications," *Mech. Syst. Signal Process.*, vol. 42, no. 1–2, pp. 314–334, 2014.
- [7] X. Li, F. Duan, D. Mba, and I. Bennett, "Multidimensional prognostics for rotating machinery: A review," *Adv. Mech. Eng.*, vol. 9, no. 2, pp. 1–20, 2017.
- [8] M. S. Kan, A. C. C. Tan, and J. Mathew, "A review on prognostic techniques for non-stationary and non-linear rotating systems," *Mech. Syst. Signal Process.*, vol. 62, pp. 1–20, 2015.
- [9] R. J. Hansen, D. L. Hall, and S. K. Kurtz, "A new approach to the challenge of machinery prognostics," *J. Eng. Gas Turbines Power*, vol. 117, no. 2, pp. 320–325, 1995.
- [10] V. T. Tran and B. S. Yang, "An intelligent condition-based maintenance platform for rotating machinery," *Expert Syst. Appl.*, vol. 39, no. 3, pp. 2977–2988, 2012.
- [11] S. T. Kandukuri, A. Klausen, H. R. Karimi, and K. G. Robbersmyr, "A review of diagnostics and prognostics of low-speed machinery towards wind turbine farm-level health management," *Renew. Sustain. Energy Rev.*, vol. 53, pp. 697–708, 2016.
- [12] M. Lebold, K. McClintic, R. Campbell, C. Byington, and K. Maynard, "Review of vibration analysis methods for gearbox diagnostics and prognostics," *54th Meet. Soc. Mach. Fail. Prev. Technol.*, no. January 1985, pp. 623–634, 2000.
- [13] J. Z. Sikorska, M. Hodkiewicz, and L. Ma, "Prognostic modelling options for remaining useful life estimation by industry," *Mech. Syst. Signal Process.*, vol. 25, no. 5, pp. 1803–1836, 2011.
- [14] S. Mathew, D. Das, R. Rossenberger, and M. Pecht, "Failure mechanisms based prognostics," no. November, 2008.
- [15] W. Tiddens, J. Braaksma, and T. Tinga, "Selecting Suitable Candidates for Predictive Maintenance," *Int. J. Progn. Heal. Manag.*, vol. 9, no. May, p. 14, 2018.
- [16] R. Xu and Y. Liu, "Failure Modes Mechanisms Effects Analysis for Refrigeration Device," vol. 288, pp. 69–74, 2013.
- [17] M. Brahimi, K. Medjaher, M. Leouatni, and N. Zerhouni, "Development of A Prognostics and Health Management System for the Railway Infrastructure – Review and Methodology," 2016

-
- Progn. Syst. Heal. Manag. Conf.*, pp. 1–8, 2016.
- [18] J. S. Khangar VS, “A review of various methodologies used for shaft failure analysis,” *Int. J. Emerg. Technol. Adv. Eng.*, vol. 2, no. 6, pp. 50–54, 2012.
- [19] “Failure Analysis Of Machine Shafts - Efficient Plant.” .
- [20] D. C. D. Hariom, Vijoy kumar, “A Review of Fundamental Shaft Failure Analysis,” *Int. Res. J. Eng. Technol.*, pp. 389–395, 2016.
- [21] W. Schütz, “A history of fatigue,” *Eng. Fract. Mech.*, vol. 54, no. 2, pp. 263–300, 1996.
- [22] W. Cui, “A state-of-the-art review on fatigue life prediction methods for metal structures,” *J. Mar. Sci. Technol.*, vol. 7, no. 1, pp. 43–56, 2002.
- [23] H. Jahed and A. Varvani-Farahani, “Upper and lower fatigue life limits model using energy-based fatigue properties,” *Int. J. Fatigue*, vol. 28, no. 5–6, pp. 467–473, 2006.
- [24] M. Kamal and M. M. Rahman, “Advances in fatigue life modeling: A review,” *Renew. Sustain. Energy Rev.*, vol. 82, no. August 2015, pp. 940–949, 2018.
- [25] P. Smith, K.N., Topper, T.H., Watson, “A stress–strain function for the fatigue of metals (stress-strain function for metal fatigue including mean stress effect),” *J Mater.*, vol. 5, no. January 1970, pp. 767–778, 1970.
- [26] A. Fatemi and L. Vangt, “Cumulative fatigue damage and life,” vol. 20, no. 1, pp. 9–34, 1998.
- [27] S. Silitonga, J. Maljaars, F. Soetens, and H. H. Snijder, “Survey on damage mechanics models for fatigue life prediction,” *Heron*, vol. 58, no. 1, pp. 25–60, 2013.
- [28] J. L. Chaboche and P. M. Lesne, “a Non-Linear Continuous Fatigue Damage Model,” *Fatigue Fract. Eng. Mater. Struct.*, vol. 11, no. 1, pp. 1–17, 1988.
- [29] D. D. L., McDowell, and R. Ellis, *Advances in Multiaxial Fatigue*. ASTM International, 1993.
- [30] A. Abou Jaoude, “Analytic and linear prognostic model for a vehicle suspension system subject to fatigue,” *Syst. Sci. Control Eng.*, vol. 3, no. 1, pp. 81–98, 2015.
- [31] Zhuang and Swannson, “TMF life prediction - a critical review.pdf.” DSTO Aeronautical and Maritime research laboratory, Melbourne, p. 35, 1998.
- [32] U. of C. Socie, Darrell (PhD Theoretical and Applied Mechanics, University of Illinois at Urbana-Champaign. BS and MS, Metallurgical Engineering and U. of M. Malton, Gary (BSc (Hons) Aeronautical Engineering, “eFatigue - Thermal Mechanical Technical Background.” .
- [33] D. Liu and D. J. Pons, “A Unified Creep-Fatigue Equation with Application to Engineering Design,” *Creep*, 2018.
- [34] Manson, Halford, and Hirschberg, “CREEP-FATIGUE ANALYSIS BY STRAIN-RANGE PARTITIONINGTitle,” 1971.
- [35] J. Fu, H. Li, C. Lei, G. W. Zheng, T. J. Bian, and L. H. Zhan, “Role of thermal-mechanical loading sequence on creep aging behaviors of 5A90 Al-Li alloy,” *J. Mater. Process. Technol.*, vol. 255, no. June 2017, pp. 354–363, 2018.
- [36] H. J. Christ, A. Jung, H. J. Maier, and R. Teteruk, “Thermomechanical fatigue - Damage mechanisms and mechanism-based life prediction methods,” *Sadhana - Acad. Proc. Eng. Sci.*, vol. 28, no. 1–2, pp. 147–165, 2003.
- [37] L. Jacobsson, C. Persson, and S. Melin, “Thermo-mechanical fatigue crack propagation
-

-
- experiments in IN718," *17th Eur. Conf. Fract. 2008 Multilevel Approach to Fract. Mater. Components Struct.*, vol. 2, no. 8–9, pp. 1397–1404, 2008.
- [38] N. O. Larrosa, R. Akid, and R. A. Ainsworth, "Corrosion-fatigue: a review of damage tolerance models," *Int. Mater. Rev.*, vol. 63, no. 5, pp. 283–308, 2018.
- [39] Q. Y. Wang, R. M. Pidaparti, and M. J. Palakal, "Comparative study of corrosion-fatigue in aircraft materials," *AIAA J.*, vol. 39, no. 2, pp. 325–330, 2001.
- [40] F. Lanoue, A. Vadean, and B. Sanschagrin, "Finite element analysis and contact modelling considerations of interference fits for fretting fatigue strength calculations," *Simul. Model. Pract. Theory*, vol. 17, no. 10, pp. 1587–1602, 2009.
- [41] S. Naboulsi and J. Calcaterra, "Fretting fatigue investigation of dovetail," *11th Int. Conf. Fract. 2005, ICF11*, vol. 4, pp. 2746–2751, 2005.
- [42] T. Hattori, V. T. Kien, and M. Yamashita, "Fretting fatigue life estimations based on fretting mechanisms," *Tribol. Int.*, vol. 44, no. 11, pp. 1389–1393, 2011.
- [43] S. A. Namjoshi, S. Mall, V. K. Jain, and O. Jin, "Fretting fatigue crack initiation mechanism in Ti-6Al-4V," *Fatigue Fract. Eng. Mater. Struct.*, vol. 25, no. 10, pp. 955–964, 2002.
- [44] L. Limmer, D. Nowell, and D. A. Hills, "A combined testing and modelling approach to the prediction of the fretting fatigue performance of splined shafts," *Proc. Inst. Mech. Eng. Part G J. Aerosp. Eng.*, vol. 215, no. 2, pp. 105–112, 2001.
- [45] D. A. Hills and D. Nowell, "Mechanics of fretting fatigue - Oxford's contribution," *Tribol. Int.*, vol. 76, pp. 1–5, 2014.
- [46] O. J. McCarthy, J. P. McGarry, and S. B. Leen, "Micro-mechanical modelling of fretting fatigue crack initiation and wear in Ti-6Al-4V," *Int. J. Fatigue*, vol. 62, pp. 180–193, 2014.
- [47] T. Dick, S. Basseville, and G. Cailletaud, "Fatigue modelling in fretting contact with a crystal plasticity model," *Comput. Mater. Sci.*, vol. 43, no. 1, pp. 36–42, 2008.
- [48] S. Faanes, "Inclined cracks in fretting fatigue," *Eng. Fract. Mech.*, vol. 52, no. 1, pp. 71–82, 1995.
- [49] J. J. Madge, S. B. Leen, and P. H. Shipway, "A combined wear and crack nucleation-propagation methodology for fretting fatigue prediction," *Int. J. Fatigue*, vol. 30, no. 9, pp. 1509–1528, 2008.
- [50] E. Giner, N. Sukumar, F. D. Denia, and F. J. Fuenmayor, "Extended finite element method for fretting fatigue crack propagation," *Int. J. Solids Struct.*, vol. 45, no. 22–23, pp. 5675–5687, 2008.
- [51] C. D. Lykins, S. Mall, and V. Jain, "A shear stress-based parameter for fretting fatigue crack initiation," *Fatigue Fract. Eng. Mater. Struct.*, vol. 24, no. 7, pp. 461–473, 2001.
- [52] M. Helmi Attia, "Fretting fatigue and wear damage of structural components in nuclear power stations-Fitness for service and life management perspective," *Tribol. Int.*, vol. 39, no. 10, pp. 1294–1304, 2006.
- [53] D. Šeruga, M. Fajdiga, and M. Nagode, "Creep damage calculation for thermo mechanical fatigue," *Stroj. Vestnik/Journal Mech. Eng.*, vol. 57, no. 5, pp. 371–378, 2011.
- [54] ABO EL ATA MM and FINNIE I, "Study of creep damage rules," *ASME Pap 71-WA/Met-1*, pp. 533–541, 1971.
-

-
- [55] R. N. Ghosh, "Creep life predictions of engineering components: Problems & prospects," *Procedia Eng.*, vol. 55, pp. 599–606, 2013.
- [56] A. Syed, "Accumulated creep strain and energy density based thermal fatigue life prediction models for SnAgCu solder joints," *Proc. - Electron. Components Technol. Conf.*, vol. 1, pp. 737–746, 2004.
- [57] F. A. Leckie and D. R. Hayhurst, "Constitutive equations for creep rupture," *Acta Metall.*, vol. 25, no. 9, pp. 1059–1070, 1977.
- [58] R. Society and P. Sciences, "Geological Faults : Fracture , Creep and Strain Author (s): G . C . P . King Source : Philosophical Transactions of the Royal Society of London . Series A , Mathematical and Physical Sciences , Vol . 288 , No . 1350 , Creep of Engineering Materials and ," vol. 288, no. 1350, pp. 197–212, 2019.
- [59] M. Yatomi, K. M. Nikbin, and N. P. O'Dowd, "Creep crack growth prediction using a damage based approach," *Int. J. Press. Vessel. Pip.*, vol. 80, no. 7–8, pp. 573–583, 2003.
- [60] R. Viswanathan, "Creep Life Prediction," *Encycl. Mater. Sci. Technol.*, pp. 1782–1787, 2001.
- [61] S. G. R. Brown, R. W. Evans, and B. Wilshire, "Creep strain and creep life prediction for the cast nickel-based superalloy IN-100," *Mater. Sci. Eng.*, vol. 84, no. C, pp. 147–156, 1986.
- [62] S. Hore and R. N. Ghosh, "Computer simulation of the high temperature creep behaviour of Cr-Mo steels," *Mater. Sci. Eng. A*, vol. 528, no. 19–20, pp. 6095–6102, 2011.
- [63] Q. Meng and Z. Wang, "Creep damage models and their applications for crack growth analysis in pipes: A review," *Eng. Fract. Mech.*, vol. 205, pp. 547–576, 2019.
- [64] M. Pecht and Jie Gu, "Physics-of-failure-based prognostics for electronic products," *Trans. Inst. Meas. Control*, vol. 31, no. 3–4, pp. 309–322, 2009.
- [65] V. Atamuradov, K. Medjaher, P. Dersin, B. Lamoureux, and N. Zerhouni, "Prognostics and Health Management for Maintenance Practitioners - Review , Implementation and Tools Evaluation," no. December, 2017.
- [66] D. B. FLANAGAN, "Torque Measurements on Rotating Shafts," *Nav. Eng. J.*, vol. 74, no. 4, pp. 697–710, 1962.
- [67] M. Hilal Muftah, M. Mohamed Haris, K. Petroczki, and E. Awad Khidir, "An improved strain gauge-based dynamic torque measurement method," *Int. J. Circuits, Syst. Signal Process.*, vol. 7, no. 1, pp. 66–73, 2013.
- [68] a Lonsdale *et al.*, "Dynamic Rotary Torque Measurement Using Surface Acoustic Waves Sensor," *Exp. Fluids*, vol. 20, no. 1, pp. 697–710, 1962.
- [69] C. Motions, "Torque_Measurement_With_Angle_Sensors.pdf." Celera, A novanta company.
- [70] Honeywell, "Ways to Measure the Force Acting on a Rotating Shaft." 2018.
- [71] F. Mevissen and M. Meo, "A review of NDT/structural health monitoring techniques for hot gas components in gas turbines," *Sensors (Switzerland)*, vol. 19, no. 3, 2019.
- [72] S. R. Prasad and A. S. Sekhar, "Life estimation of shafts using vibration based fatigue analysis," *J. Mech. Sci. Technol.*, vol. 32, no. 9, pp. 4071–4078, 2018.
- [73] "Coal Dryer - Kilburn." .
- [74] ASM, "ASM Handbook - Castings," p. 2003, 1998.
-

References

- [75] R. Loenderslott, T. Tinga, and F. Lahuerta, "Research Projects _ Load and Structural Health Monitoring of Offshore wind turbine blades (SLOWIND) _ Department MS3." .
- [76] P. R. N. Childs, *Mechanical Design Engineering Handbook*. Butterworth-Heinemann, 2014.
- [77] K. LORAND, "High Cycle Fatigue Models Applied for Multiaxial Tension-Torsion Loading Based on a New Accuracy Assessment Parameter," *J. Eng. Stud. Res.*, vol. 18, no. 3, pp. 75–86, 2012.
- [78] J. Vogwell, "Analysis of a vehicle wheel shaft failure," *Eng. Fail. Anal.*, vol. 5, no. 4, pp. 271–277, 1998.
- [79] A. Göksenli and I. B. Eryürek, "Failure analysis of an elevator drive shaft," *Eng. Fail. Anal.*, vol. 16, no. 4, pp. 1011–1019, 2009.
- [80] S. S. H. A.-M. B. Engel, "Failure Analysis and Fatigue Life Estimation of a Shaft of a Rotary Draw Bending Machine," *Int. Sch. Sci. Res. Innov.*, vol. 11, no. 11, pp. 1785–1790, 2017.
- [81] M. Ognjanovic, A. Simonovic, M. Ristivojevic, and T. Lazovic, "Research of rail traction shafts and axles fractures towards impact of service conditions and fatigue damage accumulation," *Eng. Fail. Anal.*, vol. 17, no. 7–8, pp. 1560–1571, 2010.

Appendices

Appendix A Page 1

Model number	CL1	CL2	CL3	CL4	CL5	CL6	CL7	CL8	CL9	CL10	CL11	CL12	CL13	CL14	CL15	CL16	CL17	CL18	CL19	CL20	CL21	CL22	CL23
Variables																							
Stress amplitude	x	x					x		x														
Octahedral shear stress										x	x											x	
Hydrostatic stress										x	x											x	x
Shear stress												x						x	x				
Normal stress												x	x		x	x	x	x				x	
Plastic strain			x																				
Total strain (elastic+plastic)				x	x	x		x															
Shear strain												x	x		x	x	x	x	x	x	x		
Normal strain												x		x				x				x	
Normal strain excursion between two turning points of maximum shear strain													x							x	x		
Deviatoric stress amplitude																							x
Constants																							
Fatigue strength coefficient		x		x				x					x	x	x	x		x		x	x		
Fatigue strength exponent		x		x				x		x	x	x	x	x	x	x		x		x	x		
Fatigue ductility coefficient			x	x	x								x	x	x	x		x		x	x		
Fatigue ductility exponent			x	x									x	x	x	x		x		x	x		
Shear fatigue strength coefficient												x					x	x	x				
Shear fatigue strength exponent																	x	x	x				
Shear fatigue ductility coefficient																	x	x	x				
Shear fatigue ductility exponent																	x	x	x				
Shear modulus																	x	x	x				
Elastic modulus				x	x	x		x					x		x	x		x		x	x		
Yield strength																x	x					x	
Ultimate tensile strength					x		x		x														x
Octahedral shear strength coefficient										x	x												
Sines constant(alpha)										x	x												
Findley's constant(k)												x											
SN plot	x																						
Brinell hardness						x																	
Poisson ratio								x															
Elastic Poisson ratio														x		x							
Plastic Poisson ratio														x		x							
Effective Poisson ratio																				x			
Fatigue limit							x		x														x
Equivalent shear strain connection														x									
Other experimental constants							x	x	x	x	x	x	x	x		x	x					x	x
Feasible conditions																							
Uniaxial loading	x	x	x	x	x	x	x	x	x														
Multiaxial proportional loading										x	x	x	x	x	x	x	x	x	x	x	x	x	x
Multiaxial non-proportional loading											x	x	x	x	x	x	x	x	x	x	x	x	x
Material - metals	x	x	x	x	x	x	x	x	x	x	x	x	x	x	x	x	x	x	x	x	x	x	x
Material - fibre reinforced composites	x	x																					
Notes																							
Could also be used in critical plane analysis												x	x	x	x	x	x	x	x	x	x		
No need to find separate damage estimator							x	x	x														x

Table 1 FM1CL (FATIGUE-CUMULATIVE LIFE MODELS)

Appendix A Page 2

Model number	DE1	DE2	DE3	DE4	DE5	DE6	DE7	DE8	DE9	DE10	DE11	DE12	DE13	DE14	DE15	DE16	DE17
Variables																	
Number of cycles applied at particular stress level	x		x	x	x	x										x	x
Number of cycles to fail at particular stress level	x		x	x	x	x										x	x
Instantaneous stress endurance limit ratio							x										
Instantaneous strain endurance limit ratio								x									
Applied stress ratio							x										
Critical endurance limit ratio							x										
Cycle ratio							x	x	x	x	x			x			
Applied maximum cyclic strain								x									
Stress amplitude		x									x				x		
Elastic strain		x															
Plastic strain		x									x		x				
Total shear strain range									x	x							
Cyclic hardening rate											x						
Surface layer stress												x					
Constants																	
Initial strain endurance limit								x									
Critical strain endurance limit								x									
Initial stress endurance limit							x										
Critical stress endurance limit							x										
Fracture ductility							x	x									
Reference shear strain range									x	x							
Shear fatigue strength									x	x							
Cyclic strain hardening exponent											x						
Cyclic strain hardening coefficient											x						
Fatigue strength coefficient		x															
Fatigue strength exponent		x													x		
Fatigue ductility coefficient		x															
Fatigue ductility exponent		x													x		
Elastic modulus		x															
Critical stress												x					
Ultimate tensile strength																x	x
Other experimental constants			x	x	x	x	x	x	x	x	x	x	x	x			
Feasible conditions																	
Material - metals	x	x	x	x	x	x	x	x	x	x	x	x	x	x	x		
Material - fibre reinforced composites	x															x	x
Non inclusion of load sequence effects	x	x															
Inclusion of load sequence effects			x	x	x	x	x	x	x	x	x	x	x	x	x	x	x

Table 2 FM1DE (FATIGUE-DAMAGE ESTIMATORS)

Appendix A Page 3

Model number	CB1	CB2	CB3	CB4	CB5	CB6	CB7	CB8	CB9	CB10	CB11	CB 12	CB 13
Variables													
Stress amplitude	x	x	x	x	x	x	x	x	x	x	x		
Crack length	x	x	x	x	x	x	x	x	x	x	x	x	x
cycle ratio									x				
Stress ratio		x	x	x	x	x	x	x		x	x		
Plastic strain range									x				
Tensile strain												x	
Shear strain												x	
Tensile stress													x
Shear stress													x
Constants													
Ultimate tensile strength							x						
Yield strength								x					
Cyclic strain hardening exponent										x			
Cyclic fatigue strength coefficient										x			
Elastic modulus					x	x	x			x			
Fatigue ductility coefficient										x			
Fracture Toughness	x	x	x	x	x	x	x	x	x	x	x	x	x
Geometry of the crack(characteristics excluding crack length)	x	x	x	x	x	x	x	x	x	x	x	x	x
Other experimental constants	x	x	x	x	x	x	x	x	x	x	x	x	x
Feasible conditions													
Material - metals	x	x	x	x	x	x	x	x	x	x	x	x	x
Material - fibre reinforced composites	x												
Uniaxial loading	x	x	x	x	x	x	x	x	x	x	x		
Multiaxial proportional loading												x	x
Multiaxial non-proportional loading												x	x
Notes													
Valid regions of crack growth	2	2	2,3	1,2,3	2	2	1,2	1,2	1,2	2	1	2	2

Table 3 FM1CB (FATIGUE-CONDITION BASED MODELS)

Appendix A Page 4

Model number	DC1	DC2	DC3	DC4	DC5	DC6	DC7	DC8	DC9	DC10	DC11	DC12	DC13	DC14	DC15	DC16	DC17	DC18	DC19	DC20	DC21	DC22	
Variables																							
Stress amplitude																							x
Principal normal stresses		x	x													x			x		x		
Octahedral shear stress	x	x	x					x	x	x													
Shear stress				x	x	x	x																
Shear stress acting on specified plane				x												x							
Normal stress acting on specified plane				x	x	x	x																
Amplitude of the second invariant of deviatoric stress tensor								x	x	x							x	x					
Hydrostatic stress								x	x	x		x											
Instantaneous shear stress											x												
Instantaneous hydrostatic stress											x												
Resolved shear stress amplitude												x											
Angle (location and in between planes)													x		x	x							
Volume at critical points													x										
Strain energy volumetric density at critical points													x										
Equivalent stress amplitude															x		x						
Static shear stress on specified plane															x								
Static normal stress on specified plane															x								
Alternating shear stress on specified plane															x								
Alternating normal stress on specified plane															x								
Critical stress intensity factor																	x						
Strain																	x						
Stress invariant																	x						
Amplitude of the third invariant of deviatoric stress tensor																	x						
Equivalent non linear stress																			x				
Stress triaxiality																					x		
Nucleation strain																					x		
Coalescence strain																					x		
Amplitude of deviatoric stress tensor(1-5)																						x	
Constants																							
Ultimate tensile strength							x																
Fatigue limit under fully reversed tension-compression				x	x	x		x		x						x		x					x
Fatigue limit under repeated tension									x	x						x							
Fatigue limit under fully reversed torsion	x	x	x	x	x	x	x	x	x	x						x		x					
Fatigue limit ratio																						x	
Volumetric mean value of strain energy volumetric density													x										
Strain volumetric energy density													x										
Strain work density														x									
Smoothing factor																					x		
Other experimental constants											x	x	x	x	x	x	x		x	x	x		
Feasible conditions																							
Uniaxial loading																							x
Multiaxial proportional loading	x	x	x	x	x	x	x	x	x	x	x	x	x	x	x	x	x	x	x	x	x	x	
Multiaxial non-proportional loading		x	x	x	x	x	x	x	x	x	x	x	x	x	x	x	x	x	x	x	x	x	
Material - metals	x	x	x	x	x	x	x	x	x	x	x	x	x	x	x	x	x	x	x	x	x	x	x
Material - fibre reinforced composites																							x

Table 4 FM1DC (FATIGUE-DAMAGE CRITERIA)

Appendix A Page 5

Model number	CB1	CB2	CB3	CB4	CB5	CB6
Variables						
Stress amplitude	x	x	x	x	x	x
Crack/Pit size	x			x		
Crack/pit depth		x	x	x	x	x
Pit radius					x	x
Cyclic frequency					x	x
Shear stress amplitude	x					
Friction stress	x					
Pitting current		x				
Constants						
Stress concentration factor	x	x	x	x	x	
Specimen thickness				x		
Crack closure factor				x		
Geometry factors (becomes default for crack growth models)	x	x	x	x	x	x
Fracture toughness	x	x	x	x	x	x
Fracture energy	x					
Atomic mass of the alloy		x	x			
Valence of the atoms		x	x			
Density of the alloy		x	x			
Other experimental constants	x	x	x	x	x	x
Feasible conditions						
Material - metals	x	x	x	x	x	x
Material - fibre reinforced composites						
Uniaxial loading	x	x	x	x	x	x
Multiaxial proportional loading						
Multiaxial non-proportional loading						

Table 5 FM2CB (CORROSION FATIGUE-CONDITION BASED MODELS)

Appendix A Page 6

Model number	CL1	CL2	CL3	CL4	CL5	CL6	CL7	CL8	CL9	CL10	CL11	CL12	CL13	CL14	CL15
Variables															
Plastic strain	x	x	x	x	x	x	x								
Elastic strain													x		
Total strain															x
Frequency/cyclic time	x	x	x		x	x	x								x
Temperature	x	x	x	x	x	x	x								x
Stress							x							x	
Tension going frequency								x							
Compression going frequency								x							
Inelastic strain								x	x			x	x	x	
Tensile creep strain										x	x				
Effective plastic strain											x				
Strain during tensile plasticity reversed by compressive plasticity												x		x	
Strain during tensile creep reversed by compressive creep												x		x	
Strain during tensile creep reversed by compressive plasticity												x		x	
Strain during tensile plasticity reversed by compressive creep												x		x	
Mechanical strain rate															x
Effective stress															x
Hydrostatic stress															x
Drag stress															x
Constants															
Fatigue ductility coefficient						x	x								x
Fatigue ductility exponent	x	x	x	x	x	x	x	x							x
Fatigue strength coefficient															x
Fatigue strength exponent															x
Elastic modulus															x
Yield strength						x									
Cyclic hardening index						x									
Reference temperature						x	x								
Reference frequency/cyclic time						x	x								
Tensile ductility									x						
Fatigue ductility											x				
Cyclic strain hardening exponent															
Cyclic strain hardening coefficient													x		
Low band creep ductility										x	x		x		
Threshold strain for oxide cracking															x
Mechanical strain range exponent															x
Thermal strain rate sensitivity exponent															x
Oxidation phasing constant															x
Diffusion coefficient for oxidation															x
Parabolic oxidation constant															x
Universal gas constant															x
Creep stress exponent															x
Scaling constant for creep															x
Stress state constant															x

Table 6 FM3CL (THERMOMECHANICAL FATIGUE-CUMULATIVE LIFE MODELS) PART 1 OF 2

Appendix A Page 7

Model number	CL1	CL2	CL3	CL4	CL5	CL6	CL7	CL8	CL9	CL10	CL11	CL12	CL13	CL14	CL15
Constants															
Hydrostatic stress sensitivity constant															x
Activation energy for oxidation															x
Activation energy for creep															x
Other experimental constants	x	x	x	x	x	x	x	x	x			x	x	x	x
Feasible conditions															
Material - metals	x	x	x	x	x	x	x	x	x	x	x	x	x	x	x
Material - fibre reinforced composites															
Uniaxial loading	x	x	x	x	x	x	x	x	x	x	x	x	x	x	
Multiaxial proportional loading															x
Multiaxial non-proportional loading															x
Notes															
Requires a temperature sensor	x	x	x	x	x	x	x								x

Table 7 FM3CL (THERMOMECHANICAL FATIGUE-CUMULATIVE LIFE MODELS) PART 2 OF 2

Model number	DE1	DE2	DE3	DE4	DE5	DE6
Variables						
Number of cycles applied at particular stress level	x					
Number of cycles to fail at particular stress level	x					
Instantaneous stress endurance limit ratio		x				
Instantaneous strain endurance limit ratio			x			
Applied stress ratio		x				
Critical endurance limit ratio		x				
Cycle ratio		x	x	x	x	x
Applied maximum cyclic strain			x			
Stress						x
Plastic strain						x
Total shear strain range				x	x	
Cyclic hardening rate						x
Constants						
Initial strain endurance limit			x			
Critical strain endurance limit			x			
Initial stress endurance limit		x				
Critical stress endurance limit		x				
Fracture ductility		x	x			
Reference shear strain range				x	x	
Shear fatigue strength				x	x	
Cyclic strain hardening exponent						x
Cyclic strain hardening coefficient						x
Other experimental constants		x	x	x	x	x
Feasible conditions						
Material - metals	x	x	x	x	x	x
Material - fibre reinforced composites						
Non inclusion of load sequence effects	x					
Inclusion of load sequence effects		x	x	x	x	x

Table 8 FM3DE (THERMOMECHANICAL FATIGUE-DAMAGE ESTIMATORS)

Appendix A Page 8

Model number	CL1
Variables	
Localized shear stress on critical plane	x
Constants	
Other experimental constants	x

Table 9 FM4CL (FRETTING FATIGUE-CUMULATIVE LIFE MODELS)

Model number	DE1
Variables	
Number of cycles applied at particular stress level	x
Number of cycles to fail at particular stress level	x
Constants	
Other experimental constants	
Feasible conditions	
Non inclusion of load/temperature sequence effects	x
Inclusion of load/temperature sequence effects	

Table 10 FM4DE (FRETTING FATIGUE - DAMAGE ESTIMATORS)

Model number	CL1	CL2	CL3
Variables			
Stress	x		
Time	x		
Temperature	x		
Accumulated creep strain per cycle		x	
Accumulated creep energy density per cycle			x
Constants			
Inverse of creep ductility		x	
Creep energy density for failure			x
Larson–Miller parameter	x		
Other experimental constants			
Feasible conditions			
Material - metals	x	x	x
Material - fibre reinforced composites	x		

Table 11 FM5CL (CREEP-CUMULATIVE LIFE MODELS)

Model number	DE1
Variables	
Time used at particular stress level	x
Time to rupture at particular stress level	x
Constants	
Other experimental constants	
Feasible conditions	
Material - metals	x
Material - fibre reinforced composites	x
Non inclusion of load/temperature sequence effects	x
Inclusion of load/temperature sequence effects	

Table 12 FM5DE (CREEP-DAMAGE ESTIMATORS)

Appendix A Page 9

Model number	CB1	CB2	CB3
Variables			
Activation energy	x	x	x
Temperature	x	x	x
Precipitate dissolving temperature		x	
Time	x		
Applied stress	x	x	x
Characteristic strain rate		x	
Inter particle spacing		x	
Normalized kinematic back stress		x	
Magnitude of burgers vector			x
Grain size			x
Constants			
Universal gas constant	x	x	x
Stress exponent	x		x
Time exponent	x		
Grain size exponent			x
Diffusion coefficient			x
Shear modulus			x
Boltzmann constant			x
Dislocation density		x	
Maximum strength of the matrix		x	
Effective modulus		x	
Other experimental constants	x	x	x
Feasible conditions			
Material - metals	x	x	x
Material - fibre reinforced composites			

Table 13 FM5CL (CREEP-CONDITION BASED MODELS)

Appendix A Page 10

Failure Mechanism	Model	Author/name of the model	Title of the primary reference	Author of the primary reference	Year	Secondary reference	Author of the secondary reference	Year
FM1	CL1	SN curve	A history of fatigue	Walter Schutz	1996	Kriifte, Beanspruchungen und Sicherheiten in den Landmaschinen. Z-VDI g0, 85-92 (1936).	Kloth and Stropfel	1936
FM1	CL2	Baquin's equation	A state-of-the-art review on fatigue life prediction methods for metal structures	Weicheng Cui	2002	The exponential law of endurance tests. Proc ASTM 10:625-630, 1910	Basquin,OH	1910
FM1	CL3	Coffin-Manson	Fatigue: a complex subject—some simple approximations	Manson,SS	1965			
FM1	CL4	Basquin and Coffin-Manson	A state-of-the-art review on fatigue life prediction methods for metal structures	Weicheng Cui	2002			
FM1	CL5	U. Muralidharan and S.S. Manson	A state-of-the-art review on fatigue life prediction methods for metal structures	Weicheng Cui	2002	A Modified Universal Slopes Equation for Estimation of Fatigue Characteristics of Metals,J Eng Mater Technol Trans ASME 110:55-58, 1988	U. Muralidharan and S.S. Manson	1988
FM1	CL6	Fatemi and Roeselle	Strain-controlled fatigue properties of steels and some simple approximations	Fatemi and Roeselle	2000			
FM1	CL7	Chaboche and Lesne	A non linear continuous fatigue damage model	Chaboche and Lesne	1987			
FM1	CL8	Peerlings	Enhanced damage modelling for fracture and fatigue	Peerlings	1999			
FM1	CL9	Dattoma and Giancane	Fatigue life prediction of notched components based on a new nonlinear Continuum Damage Mechanics model	Dattoma and Giancane	2010			
FM1	CL10	Sines	Failure of Materials Under Combined Repeated Stresses With Superimposed Static Stresses	Sines	1955			
FM1	CL11	Crossland	Advances in fatigue life modeling: A review	Kamal and Rahman	2018	Effect of large hydrostatic pressures on the torsional fatigue strength of an alloy steel	Crossland	1956
FM1	CL12	Findley	Advances in fatigue life modeling: A review	Kamal and Rahman	2018	A Theory for the Effect of Mean Stress on Fatigue of Metals Under Combined Torsion and Axial Load or Bending	Findley	1959
FM1	CL13	Brown, Miller and Kandil	Advances in fatigue life modeling: A review	Kamal and Rahman	2018	Biaxial low-cycle fatigue failure of 316 stainless steel at elevated temperatures	Brown, Miller and Kandil	1982
FM1	CL14	Wang and Brown	A path-independent parameter for fatigue under proportional and non-proportional loading	Wang and Brown	1993			
FM1	CL15	SWT model	A Stress-Strain function for the fatigue of metals	Smith, Watson and Topper	1970			
FM1	CL16	Fatemi - Socie	A critical plane approach to multiaxial fatigue damage including out of phase loading	Fatemi and Socie	1988			
FM1	CL17	Fatemi - Socie shear life properties	A critical plane approach to multiaxial fatigue damage including out of phase loading	Fatemi and Socie	1988			
FM1	CL18	Chu	Advances in fatigue life modeling: A review	Kamal and Rahman	2018	Fatigue Damage Calculation Using the Critical Plane Approach	Chu	1995
FM1	CL19	Glinka and Wang	Mean stress effects in multiaxial fatigue	Glinka and Wang	1995			
FM1	CL20	Shang and Sun	Multiaxial fatigue damage parameter and life prediction under low cycle loading for GH4169 alloy and other structural materials	Shang and Sun	2010			

Table 14 References - Part 1 of 6

Appendix A Page 11

Failure Mechanism	Model	Author/name of the model	Title of the primary reference	Author of the primary reference	Year	Secondary reference	Author of the secondary reference	Year
FM1	CL21	Li,Sun and Zhang	Multiaxial fatigue life prediction for various metallic materials based on the critical plane approach	Li,Sun and Zhang	2011			
FM1	CL22	Chaudonneret	A critical review on multiaxial fatigue assessments of metals	Bong and Soon	1996	A Simple and Efficient Multiaxial Fatigue Damage Model for Engineering Applications of Macro-Crack Initiation	Chaudonneret	1993
FM1	CL23	Mamiya and Castro	Multiaxial fatigue life estimation based on a piecewise ruled S–N surface	Mamiya and Castro	2011			
FM1	CB1	Paris and Erdogan	A Critical Analysis of Crack Propagation Laws	Paris	1963			
FM1	CB2	Walker	Review of Fatigue Crack Propagation Models for Metallic Components	Sabah	2009	The Effect of Stress Ratio During Crack Propagation and Fatigue for 2024-T3 and 7075-T6 Aluminum	Walker	1970
FM1	CB3	Forman	Study of fatigue crack initiation from flaws using fracture mechanics theory	Forman	1972			
FM1	CB4	Collipriest model	Review of Fatigue Crack Propagation Models for Metallic Components	Sabah	2009	An Experimentalist's View of the Surface Flaw Problem. Physical Problems and Computational Solutions	Collipriest model	1972
FM1	CB5	McEvily	Review of Fatigue Crack Propagation Models for Metallic Components	Sabah	2009	Phenomenological and Microstructural Aspects of Fatigue	McEvily	1974
FM1	CB6	Frost and Pook model	A fracture mechanics analysis of fatigue crack growth data for various materials	Frost and Pook	1971			
FM1	CB7	Zheng	Fatigue crack propagation in steels	Zheng	1983			
FM1	CB8	Wang	Review of Fatigue Crack Propagation Models for Metallic Components	Sabah	2009	Fatigue Crack Growth Rate of Metal by Plastic Energy Damage Accumulation Theory	Wang	1994
FM1	CB9	Miller and Gallagher	Review of Fatigue Crack Propagation Models for Metallic Components	Sabah	2009	An Analysis of Several Fatigue Crack Growth Rate (FCGR) Descriptions	Miller and Gallagher	1981
FM1	CB10	Pandey and Chand	Fatigue crack growth model for constant amplitude loading	Pandey and Chand	2004			
FM1	CB11	Frost and Dugdale	The propagation of fatigue cracks in sheet specimens	Frost and Dugdale	1958			
FM1	CB12	Nakamura	Fatigue crack initiation and growth behavior of Ti–6Al–4V under non-proportional multiaxial loading	Nakamura	2011			
FM1	CB13	M.Akama	Fatigue Crack Growth under Non-Proportional Mixed Mode Loading in Rail and Wheel Steel Part 1: Sequential Mode I and Mode II Loading	M.Akama	2019			
FM1	DC1	von Mises	Mechanik der festen Körper im plastisch- deformablen Zustand	von Mises	1913			
FM1	DC2	Bishop and Sherrat	Finite Element Based Fatigue Calculations (book)	Bishop and Sherrat	2000			
FM1	DC3	Tresca	Review of high cycle fatigue models applied for multiaxial tension-torsion loading based on a new accuracy assessment parameter	Lorand Kun	2012	Mémoire sur l'écoulement des corps solides soumis à de fortes pressions, Comptes Rendus Hebdomadaires des Seances de l'Academie des Sciences Paris, vol. 59, 1864, p. 754.	Tresca	1864

Table 15 References - Part 2 of 6

Appendix A Page 12

Failure Mechanism	Model	Author/name of the model	Title of the primary reference	Author of the primary reference	Year	Secondary reference	Author of the secondary reference	Year
FM1	DC4	Yokobori and Yoshimura	Review of high cycle fatigue models applied for multiaxial tension-torsion loading based on a new accuracy assessment parameter	Lorand Kun	2012	A criterion for fatigue fracture under multiaxial alternating stress state	Yokobori and Yoshimura	1966
FM1	DC5	Findley	Review of high cycle fatigue models applied for multiaxial tension-torsion loading based on a new accuracy assessment parameter	Lorand Kun	2012	A Theory for the Effect of Mean Stress on Fatigue of Metals Under Combined Torsion and Axial Load or Bending	Findley	1957
FM1	DC6	Matake	An explanation on fatigue limit under combined stress	Matake	1977			
FM1	DC7	McDiarmid	Review of high cycle fatigue models applied for multiaxial tension-torsion loading based on a new accuracy assessment parameter	Lorand Kun	2012	A shear stress based critical-plane criterion for multiaxial fatigue failure for design and life prediction	McDiarmid	1994
FM1	DC8	Crossland	Review of high cycle fatigue models applied for multiaxial tension-torsion loading based on a new accuracy assessment parameter	Lorand Kun	2012	Effect of large hydrostatic pressures on the torsional fatigue strength of an alloy steel	Crossland	1956
FM1	DC9	Sines	Review of high cycle fatigue models applied for multiaxial tension-torsion loading based on a new accuracy assessment parameter	Lorand Kun	2012	Behavior of metals under complex static and alternating stresses	Sines	1959
FM1	DC10	Kakuno-Kawada	A new criterion of fatigue strength of a round bar subjected to combined static and repeated bending and torsion	Kakuno-Kawada	1979			
FM1	DC11	Dang Van	Advances in fatigue life modeling: A review	Kamal and Rahman	2018	Macro-Micro Approach in High-Cycle Multiaxial Fatigue	Dang Van	1993
FM1	DC12	Papadopoulos	A new criterion of fatigue strength for out-of-phase bending and torsion of hard metals	Papadopoulos	1994			
FM1	DC13	Lasserre and Palin-Luc	An energy based criterion for high cycle multiaxial fatigue	Lasserre and Palin-Luc	1998			
FM1	DC14	Saintier and Palin-Luc	Non-local energy based fatigue life calculation method under multiaxial variable amplitude loadings	Saintier and Palin-Luc	2013			
FM1	DC15	Zenner and Simburger	On the fatigue limit of ductile metals under complex multiaxial loading	Zenner and Simburger	2000			
FM1	DC16	Papuga and Ruzicka	Two new multiaxial criteria for high cycle fatigue computation	Papuga and Ruzicka	2008			
FM1	DC17	Horstemeyer and Gokhale	A void–crack nucleation model for ductile metals	Horstemeyer and Gokhale	1999			
FM1	DC18	Vu and Halm	Multiaxial fatigue criterion for complex loading based on stress invariants	Vu and Halm	2010			
FM1	DC19	Emuakpor and George	A new distortion energy-based equivalent stress for multiaxial fatigue life prediction	Emuakpor and George	2012			
FM1	DC20	Khandelwal and El-tawil	A finite strain continuum damage model for simulating ductile fracture in steels	Khandelwal and El-tawil	2014			
FM1	DC21	Mamiya and Goncalves	Multiaxial fatigue: a stress based criterion for hard metals	Mamiya and Goncalves	2005			
FM1	DC22	Wohler	A history of fatigue	Walter Schutz	1996	Kriifte, Beanspruchungen und Sicherheiten in den Landmaschinen. Z-VDI g0, 85-92 (1936).	Kloth and Stropfel	1936

Table 16 References - Part 3 of 6

Appendix A Page 13

Failure Mechanism	Model	Author/name of the model	Title of the primary reference	Author of the primary reference	Year	Secondary reference	Author of the secondary reference	Year
FM1	DE1	Miner's LDR	A history of fatigue	Walter Schutz	1996	Cumulative damage in fatigue	Miner	1945
FM1	DE2	Landgraf	Cumulative fatigue damage and life prediction theories: a survey of the state of the art for homogeneous materials	Fatemi and Yang	1998	Cumulative Fatigue Damage Under Complex Strain Histories	Landgraf	1971
FM1	DE3	Manson	Application of a double linear damage rule to cumulative fatigue	Manson	1967			
FM1	DE4	Manson and Halford	Re-examination of cumulative fatigue damage analysis—an engineering perspective	Manson and Halford	1986			
FM1	DE5	Manson and Halford	Re-examination of cumulative fatigue damage analysis—an engineering perspective	Manson and Halford	1986			
FM1	DE6	Manson and Halford	Re-examination of cumulative fatigue damage analysis—an engineering perspective	Manson and Halford	1986			
FM1	DE7	Bui-Quoc	An interaction effect consideration in cumulative damage on a mild steel under torsion loading	Bui-Quoc	1981			
FM1	DE8	Bui-Quoc	Cumulative fatigue damage and life prediction theories: a survey of the state of the art for homogeneous materials	Fatemi and Yang	1998	Cumulative fatigue damage under strain controlled conditions	Bui-Quoc	1971
FM1	DE9	Bui-Quoc	An interaction effect consideration in cumulative damage on a mild steel under torsion loading	Bui-Quoc	1981			
FM1	DE10	Bui-Quoc	Cumulative fatigue damage and life prediction theories: a survey of the state of the art for homogeneous materials	Fatemi and Yang	1998	Cumulative damage with interaction effect due to fatigue under torsion loading	Bui-Quoc	1982
FM1	DE11	Niu theory	Hardening law and fatigue damage of a cyclic hardening metal	Niu	1987			
FM1	DE12	Kramer	Cumulative fatigue damage and life prediction theories: a survey of the state of the art for homogeneous materials	Fatemi and Yang	1998	A mechanism of fatigue failure	Kramer	1974
FM1	DE13	Azari	Cumulative fatigue damage and life prediction theories: a survey of the state of the art for homogeneous materials	Fatemi and Yang	1998	Functions of damage in low cycle fatigue	Azari	1984
FM1	DE14	Fong	Cumulative fatigue damage and life prediction theories: a survey of the state of the art for homogeneous materials	Fatemi and Yang	1998	What Is Fatigue Damage?	Fong	1982
FM1	DE15	Kurath	Cumulative fatigue damage and life prediction theories: a survey of the state of the art for homogeneous materials	Fatemi and Yang	1998	The effect of selected subcycle sequences in fatigue loading histories	Kurath	1984
FM1	DE16	Broutman-Sahu	Predicting damage accumulation in glass fiber reinforced plastics through cumulative damage models	Broutman-Sahu	2011			
FM1	DE17	Hashin-Rotem	Predicting damage accumulation in glass fiber reinforced plastics through cumulative damage models	Broutman-Sahu	2011			
FM2	CB1	Wang	Comparative Study of Corrosion–Fatigue in Aircraft Materials	Wang	2001			
FM2	CB2	Sriraman and Pidaparti	Life prediction of aircraft Aluminium subjected to pitting corrosion under fatigue conditions	Sriraman and Pidaparti	2009			

Table 17 References - Part 4 of 6

Appendix A Page 14

Failure Mechanism	Model	Author/name of the model	Title of the primary reference	Author of the primary reference	Year	Secondary reference	Author of the secondary reference	Year
FM2	CB3	Li an Akid	Corrosion fatigue life prediction of a steel shaft material in seawater	Li an Akid	2013			
FM2	CB4	Rokhlin	Effect of pitting corrosion on fatigue crack initiation and fatigue life	Rokhlin	1999			
FM2	CB5	Chen	Corrosion and corrosion fatigue of airframe aluminum alloys	Chen	1994			
FM2	CB6	Kondo	Prediction of Fatigue Crack Initiation Life Based on Pit Growth	Kondo	1989			
FM3	CL1	Coffin-Manson	A Study of the Effects of Cyclic Thermal Stresses on a Ductile Metal	Coffin-Manson	1954			
FM3	CL2	Solomon	Fatigue of 60/40 Solder	Solomon	1986			
FM3	CL3	Shi	Low cycle fatigue analysis of temperature and frequency effects ineutectic solder alloy	Shi	2000			
FM3	CL4	Jing	Low cycle fatigue behavior of a eutectic 80Au/20Sn solder alloy	Jing	2015			
FM3	CL5	Engelmaier	Fatigue Life of Leadless Chip Carrier Solder Joints During Power Cycling	Engelmaier	1983			
FM3	CL6	Wong and Mai	A unified equation for creep-fatigue	Wong and Mai	2014			
FM3	CL7	Wong,Liu and Pons	The Unified Creep-Fatigue Equation for Stainless Steel 316	Wong,Liu and Pons	2016			
FM3	CL8	Coffin-Manson	Thermo-Mechanical Fatigue Life Prediction: A Critical Review	Zhuang and Swannson	1988	Concept of frequency separation in life prediction for time-dependent fatigue	Coffin-Manson	1976
FM3	CL9	Ellison	Thermo-Mechanical Fatigue Life Prediction: A Critical Review	Zhuang and Swannson	1988	A Review of the Interaction of Creep and Fatigue	Ellison	1969
FM3	CL10	Edmunds and White	Thermo-Mechanical Fatigue Life Prediction: A Critical Review	Zhuang and Swannson	1988	Observations of the Effect of Creep Relaxation on High-Strain Fatigue	Edmunds and White	1966
FM3	CL11	Priest and Ellison	A combined deformation map-ductility exhaustion approach to creep-fatigue analysis	Priest and Ellison	1981			
FM3	CL12	Manson	Creep-Fatigue Analysis by Strainrange Partitioning	Manson	1971			
FM3	CL13	Halford and Saltsman	Strainrange Partitioning - A Total Strainrange Version	Halford and Saltsman	1983			
FM3	CL14	He	Strain energy partitioning and its application to GH33A nickel-base superalloy and 1Cr-18Ni-9Ti stainless steel	He, J	1983			
FM3	CL15	Sehitoglu	Altair efatigue	Altair	-	Thermo-Mechanical Fatigue Life Prediction Methods	Sehitoglu	1992

Table 18 References - Part 5 of 6

Appendix A Page 15

Failure Mechanism	Model	Author/name of the model	Title of the primary reference	Author of the primary reference	Year	Secondary reference	Author of the secondary reference	Year
FM3	DE1	Combination of life fraction rule and linear damage rule	A study of creep damage rules	Abo and Finnie	1972	Effect of Temperature Variation on the Creep Strength of Steels	Robinson	1938
			A history of fatigue	Walter Schutz	1996	Cumulative damage in fatigue	Miner	1945
FM3	DE2	Bui-Quoc	An interaction effect consideration in cumulative damage on a mild steel under torsion loading	Bui-Quoc	1981			
FM3	DE3	Bui-Quoc	Cumulative fatigue damage and life prediction theories: a survey of the state of the art for homogeneous materials	Fatemi and Yang	1998	Cumulative fatigue damage under strain controlled conditions	Bui-Quoc	1971
FM3	DE4	Bui-Quoc	An interaction effect consideration in cumulative damage on a mild steel under torsion loading	Bui-Quoc	1981			
FM3	DE5	Bui-Quoc	Cumulative fatigue damage and life prediction theories: a survey of the state of the art for homogeneous materials	Fatemi and Yang	1998	Cumulative damage with interaction effect due to fatigue under torsion loading	Bui-Quoc	1982
FM3	DE6	Niu theory	Hardening law and fatigue damage of a cyclic hardening metal	Niu	1987			
FM4	CL1	Lykin, Mall and Jain	A shear stress-based parameter for fretting fatigue crack initiation	Lykin, Mall and Jain	2001			
FM4	DE1	Miner	A history of fatigue	Walter Schutz	1996	Cumulative damage in fatigue	Miner	1945
FM5	CL1	Larson Miller	Creep Life Prediction ns of Engineering Components: Problems & Prospects	Ghosh	2013	A time-temperature relationship for rupture and creep stresses	Larson Miller	1952
FM5	CL2	Ahmed, Amkor	Accumulated Creep Strain and Energy Density Based Thermal Fatigue Life Prediction Models for SnAgCu Solder Joints	Ahmed, Amkor	2004			
FM5	CL3	Ahmed, Amkor 2	Accumulated Creep Strain and Energy Density Based Thermal Fatigue Life Prediction Models for SnAgCu Solder Joints	Ahmed, Amkor	2004			
FM5	DE1	Life fraction rule	A study of creep damage rules	Abo and Finnie	1972	Effect of Temperature Variation on the Creep Strength of Steels	Robinson	1938
FM5	CB1	Algebraic creep strain power laws	Creep Life Prediction ns of Engineering Components: Problems & Prospects	Ghosh	2013			
FM5	CB2	Dyson and McLean	Creep Life Prediction ns of Engineering Components: Problems & Prospects	Ghosh	2013	Use of CDM in materials modeling and component creep life prediction	Dyson	2000
FM5	CB3	Mukherjee	Experimental correlations for high temperature creep	Mukherjee	1968			

Table 19 References - Part 6 of 6

Appendix B – Ideal Guidance sheet for shaft failure mechanisms and creep

Note : NA in the following tables refers to “Not Available”

Failure mechanism	Cumulative life models		
	Feasible conditions	Models	
Fatigue (FM1)	Metals	Uniaxial loading	CL1-CL23
		Multiaxial proportional loading	CL10-CL23
		Multiaxial non-proportional loading	CL11-CL23
	Fibre reinforced composites	Uniaxial loading	CL1-CL2
		Multiaxial proportional loading	NA
		Multiaxial non-proportional loading	NA
Corrosion fatigue (FM2)	Metals	Uniaxial loading	NA
		Multiaxial proportional loading	
		Multiaxial non-proportional loading	
	Fibre reinforced composites	Uniaxial loading	
		Multiaxial proportional loading	
		Multiaxial non-proportional loading	
Thermo-mechanical fatigue (FM3)	Metals	Uniaxial loading	CL1-CL15
		Multiaxial proportional loading	NA
		Multiaxial non-proportional loading	
	Fibre reinforced composites	Uniaxial loading	
		Multiaxial proportional loading	
		Multiaxial non-proportional loading	
Fretting fatigue (FM4)	NA		
Creep (FM5)	Metals		CL1-CL3
	Fibre reinforced composites		CL1

Table 1 Guidance sheet for cumulative life models

Failure mechanism	Damage estimator		
	Feasible conditions		Models
Fatigue (FM1)	Metals	Inclusion of load sequence effects	DE3-DE15
		Non inclusion of load sequence effects	DE1-DE2
	Fibre reinforced composites	Inclusion of load sequence effects	DE16-DE17
		Non inclusion of load sequence effects	DE1
Corrosion fatigue (FM2)	Metals	Inclusion of load sequence effects	NA
		Non inclusion of load sequence effects	NA
	Fibre reinforced composites	Inclusion of load sequence effects	
		Non inclusion of load sequence effects	
Thermo-mechanical fatigue (FM3)	Metals	Inclusion of load/temperature sequence effects	
		Non inclusion of load/temperature sequence effects	DE1
	Fibre reinforced composites	Inclusion of load/temperature sequence effects	NA
		Non inclusion of load/temperature sequence effects	NA
Fretting fatigue (FM4)	NA		DE1
Creep (FM5)	Metals	Inclusion of load/temperature sequence effects	NA
		Non inclusion of load/temperature sequence effects	DE1
	Fibre reinforced composites	Inclusion of load/temperature sequence effects	NA
		Non inclusion of load/temperature sequence effects	DE1

Table 2 Guidance sheet for damage estimator

Appendix B-Page 2

Failure mechanism	Condition based models		Final threshold	
	Feasible conditions	Models		
Fatigue (FM1)	Metals	Uniaxial loading	CB1-CB11	Critical crack length
		Multiaxial proportional loading	CB12-CB13	
		Multiaxial non-proportional loading	CB12-CB13	
	Fibre reinforced composites	Uniaxial loading	CB1	
		Multiaxial proportional loading	NA	
		Multiaxial non-proportional loading	NA	
Corrosion fatigue (FM2)	Metals	Uniaxial loading	CB1-CB6	
		Multiaxial proportional loading	NA	
		Multiaxial non-proportional loading		
	Fibre reinforced composites	Uniaxial loading		
		Multiaxial proportional loading		
		Multiaxial non-proportional loading		
Thermo-mechanical fatigue (FM3)	NA			NA
Fretting fatigue (FM4)	NA		NA	Critical crack length
Creep (FM5)	Metals		CB1-CB3	Percentage of strain
	Fibre reinforced composites		NA	

Table 3 Guidance sheet for condition based models and final threshold

Failure mechanism	Damage criteria		
	Feasible conditions		Models
Fatigue (FM1)	Metals	Uniaxial loading	DC1-DC22
		Multiaxial proportional loading	DC1-DC21
		Multiaxial non-proportional loading	DC2-DC21
	Fibre reinforced composites	Uniaxial loading	NA
		Multiaxial proportional loading	NA
		Multiaxial non-proportional loading	NA
Corrosion fatigue (FM2)	NA	NA	NA
Thermo-mechanical fatigue (FM3)	NA	NA	NA
Fretting fatigue (FM4)	NA	NA	NA
Creep (FM5)	NA	NA	NA

Table 4 Guidance sheet for damage criteria

Appendix C Page 1

Simplification of variables and matching them with the sensors

Failure mechanism and model type	Loading scenario/any criteria	Variables from the possible models for the respective loading scenarios	Possible manifestations in the shaft required	Requirements, if it is not possible to manifest	Possible sensors
Fatigue - FM1 (Cumulative life models)	Pure bending (uniaxial tensile)	Stress amplitude	Bending stress		Strain gauge rosette/Vibration sensor
		Normal stress	Bending stress		Strain gauge rosette/Vibration sensor
		Plastic strain	Plastic portion of bending strain		Strain gauge rosette
		Total strain (elastic+plastic)	Bending strain		Strain gauge rosette
	Pure torsion (Shear)	Stress amplitude	Shear stress		Strain gauge rosette/Torque cell
		Plastic strain	Plastic portion of shear strain		Strain gauge rosette
		Total strain (elastic+plastic)	Shear strain		Strain gauge rosette
	Combined bending and torsion (multiaxial non-proportional)	Octahedral shear stress	Stress tensor (Bending stress and shear stress)		Strain gauge rosette/Torque cell
		Hydrostatic stress	Stress tensor (Bending stress)		Strain gauge rosette/Torque cell
		Shear stress	Shear stress		Strain gauge rosette/Torque cell
		Normal stress	Principal stress (Bending stress and shear stress)		Strain gauge rosette/Torque cell
		Shear strain	Shear strain		Strain gauge rosette
		Normal strain	Principal normal strain (Bending strain and shear strain)		Strain gauge rosette
Normal strain excursion between two turning points of maximum shear strain			Critical plane analysis	Not feasible with available sensors	
Deviatoric stress amplitude	Stress tensor (Bending stress and shear stress)		Strain gauge rosette/Torque cell		
Fatigue - FM1 (Damage estimators)	Not applicable	Number of cycles applied at particular stress level		Counting	Not required
		Number of cycles to fail at particular stress level		Estimated from cumulative life models	Not required
		Instantaneous stress endurance limit ratio	Bending stress/shear stress		With respect to stress used in cumulative life model
		Instantaneous strain endurance limit ratio	Bending strain/shear strain		With respect to strain used in cumulative life model
		Applied stress ratio	Bending stress/shear stress		With respect to stress used in cumulative life model
		Critical endurance limit ratio	Bending stress/shear stress		With respect to strain used in cumulative life model
		Cycle ratio		Counting	Not required
		Applied maximum cyclic strain	Bending strain/shear strain		With respect to strain used in cumulative life model
		Stress	Bending stress/shear stress		With respect to stress used in cumulative life model
		Elastic strain	Elastic portion of bending strain/shear strain		With respect to strain used in cumulative life model
		Plastic strain	Plastic portion of bending strain/shear strain		With respect to strain used in cumulative life model
		Total shear strain range	Shear strain		Strain gauge rosette
		Cyclic hardening rate	Strain hardening		Not feasible with available sensors
		Surface layer stress	Surface layer stress		Not feasible with available sensors
Fatigue - FM1 (Condition based models)	Pure bending (uniaxial tensile)/Torsion (Shear stress)	Stress amplitude	Bending stress/shear stress		Strain gauge rosette/Torque cell/vibration sensor
		Crack length	crack length		Not feasible with available sensors
		cycle ratio		Counting	Not required
		Stress ratio	Bending stress/shear stress		Not required
		Plastic strain range	Plastic portion of bending strain/shear strain		Strain gauge rosette

Appendix C Page 2

Failure mechanism and model type	Loading scenario/any criteria	Variables from the possible models for the respective loading scenarios	Possible manifestations in the shaft required	Requirements, if it is not possible to manifest	Possible sensors	
Fatigue - FM1 (Damage criteria)	Pure bending (uniaxial tensile)	Stress amplitude	Bending stress		Strain gauge rosette/Vibration sensor	
	Pure torsion (Shear)	Stress amplitude	Shear stress		Strain gauge rosette/Torque cell	
	Combined bending and torsion (multiaxial non-proportional)	Principal normal stresses	Principal stress (Bending stress and shear stress)			Strain gauge rosette/Torque cell
		Octahedral shear stress	Stress tensor (Bending stress and shear stress)			Strain gauge rosette/Torque cell
		Shear stress	Shear stress			Strain gauge rosette/Torque cell
		Shear stress acting on specified plane		Critical plane analysis		Not feasible with available sensors
		Normal stress acting on specified plane		Critical plane analysis		Not feasible with available sensors
		Hydrostatic stress	Stress tensor (Bending stress)			Strain gauge rosette/Torque cell
		Instantaneous shear stress	Shear stress			Strain gauge rosette/Torque cell
		Instantaneous hydrostatic stress	Stress tensor (Bending stress)			Strain gauge rosette/Torque cell
		Resolved shear stress amplitude	Shear stress			Strain gauge rosette/Torque cell
		Angle (location and in between planes)		Critical plane analysis		Not feasible with available sensors
		Volume at critical points		FE solving		Not feasible with available sensors
		Strain energy volumetric density at critical points		FE solving		Not feasible with available sensors
		Equivalent stress amplitude	Bending stress/shear stress			Strain gauge rosette/Torque cell
		Static shear stress on specified plane		Critical plane analysis		Not feasible with available sensors
		Static normal stress on specified plane		Critical plane analysis		Not feasible with available sensors
		Alternating shear stress on specified plane		Critical plane analysis		Not feasible with available sensors
		Alternating normal stress on specified plane		Critical plane analysis		Not feasible with available sensors
		Critical stress intensity factor	Bending stress/shear stress			Strain gauge rosette/Torque cell
		Strain	Bending strain/shear strain			Strain gauge rosette
		Stress invariant	Stress tensor (Bending stress and shear stress)			Strain gauge rosette/Torque cell
		Amplitude of the third invariant of deviatoric stress tensor	Stress tensor (Bending stress and shear stress)			Strain gauge rosette/Torque cell
		Equivalent non linear stress	Non linear part of bending/shear stress			Strain gauge rosette/Torque cell
		Stress triaxiality	Stress tensor (Bending stress and shear stress)			Strain gauge rosette/Torque cell
		Nucleation strain		Microscopic level		Not feasible with available sensors
	Coalescence strain		Microscopic level		Not feasible with available sensors	
	Amplitude of invariants of deviatoric stress tensor	Stress tensor (Bending stress and shear stress)			Strain gauge rosette/Torque cell	
	Corrosion fatigue - FM2 (Condition based models)	Pure bending (uniaxial tensile)/Torsion (Shear stress)	Stress amplitude	Bending stress/shear stress		Strain gauge rosette/Torque cell/vibration sensor
			Crack/Pit size	Crack/Pit size		Not feasible with available sensors
Crack/pit depth			Crack/pit depth		Not feasible with available sensors	
Pit radius			Pit radius		Not feasible with available sensors	
Shear stress amplitude			Shear stress		Strain gauge rosette/Torque cell	
Friction stress					Not required	
Cyclic frequency				Counting	Not required	
Pitting current			Current		Electrochemical cell	
Cyclic frequency				Counting	Not required	

Appendix C Page 3

Failure mechanism and model type	Loading scenario/any criteria	Variables from the possible models for the respective loading scenarios	Possible manifestations in the shaft required	Requirements, if it is not possible to manifest	Possible sensors
Corrosion fatigue (Damage estimator)	Not applicable	Number of cycles applied at particular stress level		Counting	Not required
		Number of cycles to fail at particular stress level		Estimated from cumulative life models	Not required
Thermo-mechanical fatigue - FM3 (Cumulative life models)	Pure bending (uniaxial tensile)/Torsion (Shear stress)	Plastic strain	Plastic portion of bending strain/shear strain		Strain gauge rosette
		Elastic strain	Elastic portion of bending strain/shear strain		Strain gauge rosette
		Frequency/cyclic time		Counting	Not required
		Temperature	Temperature		Pyrometer/Thermocouple
		Stress	Bending stress/shear stress		Strain gauge rosette/Torque cell/vibration sensor
		Tension going frequency		Counting	Not required
		Compression going frequency		Counting	Not required
		Inelastic strain	Plastic portion of bending strain/shear strain		Strain gauge rosette
		Tensile creep strain	Plastic portion of bending strain at high temperature		Strain gauge rosette
		Effective plastic strain	Plastic portion of bending strain/shear strain		Strain gauge rosette
		Strain during tensile plasticity reversed by compressive plasticity	Strain partitioning of bending/shear strain		Not feasible with available sensors
		Strain during tensile creep reversed by compressive creep	Strain partitioning of bending/shear strain		Not feasible with available sensors
	Strain during tensile creep reversed by compressive plasticity	Strain partitioning of bending/shear strain		Not feasible with available sensors	
	Strain during tensile plasticity reversed by compressive creep	Strain partitioning of bending/shear strain		Not feasible with available sensors	
	Combined bending and torsion (multiaxial non-proportional)	Total strain	Bending/shear strain		Strain gauge rosette
		Frequency/cyclic time		Counting	Not required
		Temperature	Temperature		Pyrometer/Thermocouple
		Mechanical strain rate	Bending/shear strain		Strain gauge rosette
Effective stress		Bending/shear stress		Strain gauge rosette/Torque cell/vibration sensor	
Hydrostatic stress		Stress tensor(Bending stress)		Strain gauge rosette/vibration sensor	
	Drag stress		Microscopic level	Not feasible with available sensors	
Thermo-mechanical fatigue(Damage estimators)	Not applicable	Number of cycles applied at particular stress level		Counting	Not required
		Number of cycles to fail at particular stress level		Estimated from cumulative life models	Not required
		Instantaneous stress endurance limit ratio	Bending stress/shear stress		With respect to stress used in cumulative life model
		Instantaneous strain endurance limit ratio	Bending strain/shear strain		With respect to strain used in cumulative life model
		Applied stress ratio	Bending stress/shear stress		With respect to stress used in cumulative life model
		Critical endurance limit ratio	Bending stress/shear stress		With respect to stress used in cumulative life model
		Cycle ratio		Counting	Not required
		Applied maximum cyclic strain	Bending strain/shear strain		With respect to strain used in cumulative life model
		Stress	Bending stress/shear stress		With respect to stress used in cumulative life model
		Plastic strain	Plastic portion of bending strain/shear strain		Strain gauge rosette
		Total shear strain range	Shear strain		Strain gauge rosette
	Cyclic hardening rate	Strain hardening		Not feasible with available sensors	

Appendix C Page 4

Failure mechanism and model type	Loading scenario/any criteria	Variables from the possible models for the respective loading scenarios	Possible manifestations in the shaft required	Requirements, if it is not possible to manifest	Possible sensors
Fretting fatigue - FM4 (Cumulative life models)	Not applicable	Localized shear stress on critical plane		Critical plane analysis	Not feasible with available sensors
Fretting fatigue - FM4 (Damage estimators)	Not applicable	Number of cycles applied at particular stress level		Counting	Not required
		Number of cycles to fail at particular stress level		Estimated from cumulative life models	Not required

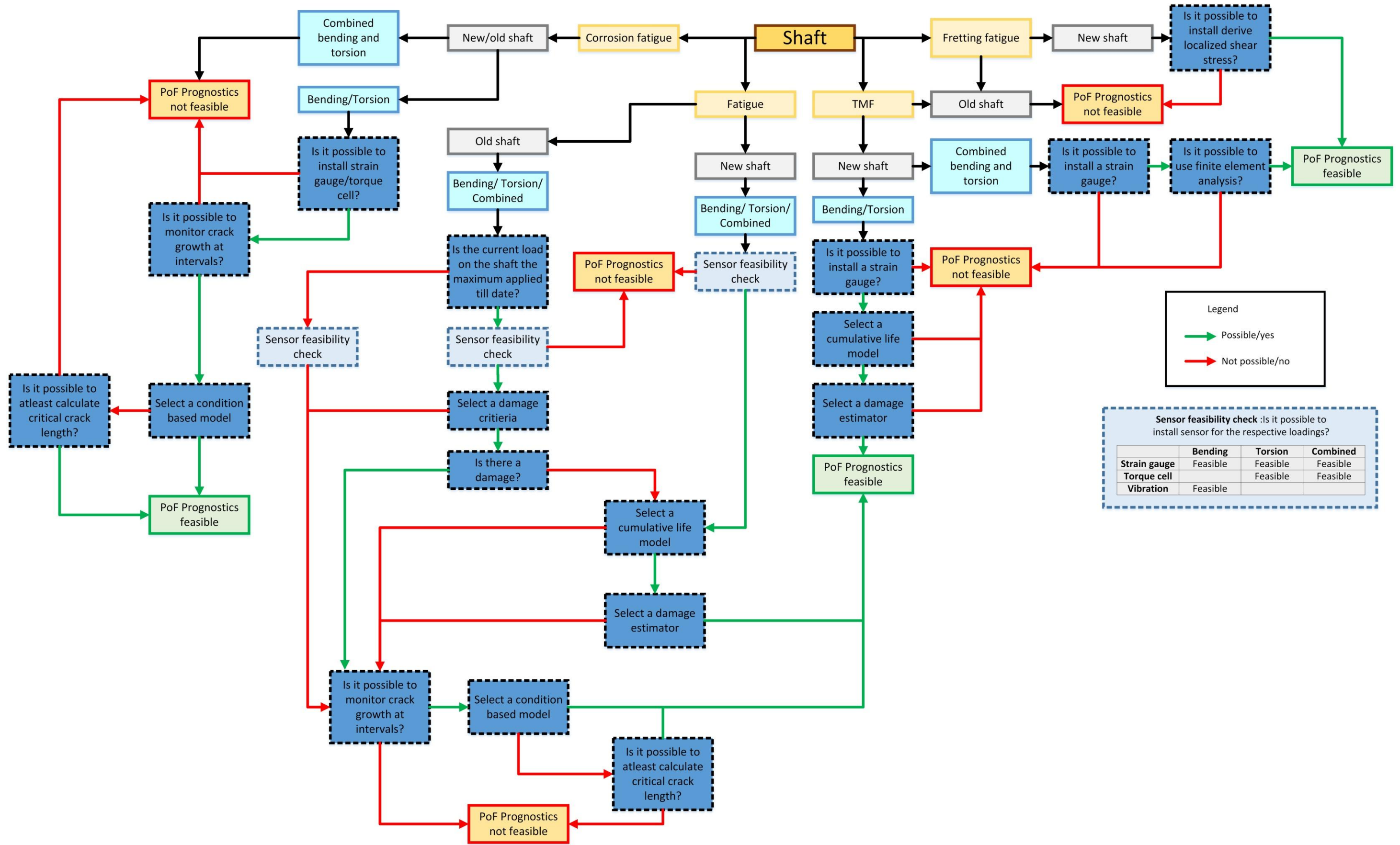


Figure 1 Customized feasibility flowchart for shaft (Revised)

Appendix D Page 2

Model	Failure mechanism	Configuration	Strain gauge rosettes	Torque cells	Vibration sensors	Pyrometer/ thermo-couple	Without sensor	Finite element analysis	Crack growth monitoring	Localized shear stress
Cumulative life model (CL)	Fatigue (FM1)	Bending	CL1-CL9		CL1, CL2, CL7, CL9					
		Torsion	CL1-CL9	CL1, CL2, CL7, CL9						
		Combined bending and torsion	CL11-CL13, CL15-CL19, CL22-CL23	CL12, CL22, CL23			CL14, CL20, CL21			
	TMF (FM3)	Bending	CL1-CL11, CL13				CL1-CL7			
		Torsion	CL1-CL11, CL13				CL1-CL7			
		Combined bending and torsion						CL15		
	Fretting fatigue (FM4)	Not Applicable								CL1
Damage estimator (DE)	Fatigue (FM1)	Not applicable	DE2,DE7-DE10, DE13-DE15	DE3-DE7, DE14-DE15	DE3-DE7, DE14-DE15		DE1,DE3-DE6			
	TMF (FM3)	Not applicable	DE2-DE6	DE2	DE2					
Damage criteria (DC)	Fatigue (FM1)	Bending	DC22		DC22					
		Torsion	DC22	DC22						
		Combined bending and torsion	DC2-DC3, DC8-DC11, DC17-DC19, DC21	DC2-DC3, DC8-DC11, DC18-DC19, DC21						
Condition based models (CB)	Fatigue (FM1)	Bending	CB1-CB11		CB11-CB11				CB1-CB11	
		Torsion	CB1-CB11	CB1-CB11					CB1-CB11	
		Combined bending and torsion	CB12-CB13	CB13					CB12-CB13	
	Corrosion fatigue (FM2)	Bending	CB1-CB6						CB1-CB6	
		Torsion	CB1-CB6	CB1-CB6					CB1-CB6	

Table 1 Guidance Sheet for shaft - Revised